ストラテラカプセル及びストラテラ内用液にて検出された新規ニトロソアミンの限度値について

日本イーライリリー株式会社及びEli Lilly and Company（以下、Lilly）はストラテラカプセル及びストラテラ内用液にて検出された N-ニトロソアトモキセチンに対して、証拠の重み付けによるアプローチを使用して、4400 ng /day を安全で適切な 許容摂取量であると判断した。この証拠の重み付けによるアプローチにおいて、Lilly は以下の 4 項目を用いている。

- ニトロソアミン類の既知の作用機序
- 物理的化学的特性に基づくリードアクロス（Jolly et al 2024）
- 量子力学モデル（De et al 2024）及び QSARFlex 等の In silico モデル（Jolly et al 2024）
- In vivo 遺伝子突然変異試験（Jolly et al 2024）

許容摂取量 4400 ng/day を支持する主要なデータである In vivo 遺伝子突然変異試験の結果については、以下に要約を記載する。また、許容摂取量 4400 ng/day を支持するその他のデータを含む参考文献（Jolly et al 2024 及び De et al 2024）についても併せて提示する。

N-ニトロソアトモキセチンは In vivo 変異原性の観点から、他のより強力なニトロソアミン類とは明確に区別されるということが特に重要であり、このことはリードアクロス分析によっても支持されている。N-ニトロソアトモキセチンは他のより強力なニトロソアミン類のように ICH M7（R2）で特定されている cohort of concern には該当しない。ICH M7（R2）では、発がん性データがなく、cohort of concern に該当しない変異原性不純物の毒性学的懸念の閾値（TTC）として、生涯曝露を考慮して 1.5 µg/day（1500 ng/day）を正当化している。当該 TTC においては、発がんリスクは無視できる程度の増加であり、過剰発がんリスクは生涯曝露において 10 万分の 1 未満として定義されている。その考えに基づいて、1500 ng/day を AI として設定することは科学的にも合理的な考え方である。

<u>In vivo 遺伝子変異試験の結果概要：</u>

Ames 試験において陽性である N-ニトロソアトモキセチンについて、トランスジェニックラットを用いた in-vivo 遺伝子変異試験を OECD 試験ガイドライン及び GLP の要求事項に従って実施した。その結果、N-ニトロソアトモキセチンは、cII 遺伝子の変異頻度を、十二指腸組織において 100 mg/kg/day、肝臓において 30 mg/kg/day 以上の用量で増加させることが示された。一方で 0.1、0.537、5 mg/kg/day の低い用量では肝臓における変異頻度は増加せず、用量反応関係における「閾値」が示された。in vivo 遺伝子変異試験における無影響量（NOEL）は 5 mg/kg/day であり、ベンチマーク用量信頼区間の下限値（BMDL；データ解析に対する十分に検証されたベンチマーク用量アプローチに基づく）は 4.4 mg/kg/day であった。許容摂取量 4400 ng/day は腫瘍発生率が 50%となる用量 TD_{50} の代わりに ICH M7（R2）の原理に基づき、BMDL の値を保守的に用いて設定した［ICH M7（R2）注 4］。

Lilly は許容摂取量の算出に関するメカニズムベースのリスク評価手法は、以下に記載するとおり科学的に妥当性が保証された方法であると考える。

- 突然変異を評価することは、ニトロソアミンの発がん性リスクを評価する上で、適切かつ十分な感度を有する評価項目である。
- トランスジェニックげっ歯類モデルは、in vivo で変異原性を評価するための堅牢で十分に検証されたモデルである。

さらに、in vivo 変異原性試験結果から得られた NOEL 及び BMDL から算出された許容摂取量は、以下の理由からより保守的な推定値であると考える。

- 変異原性ニトロソアミンによる発がん性を予測するために必要とされる評価項目であり、腫瘍を評価項目とすることよりも保守的である。
- NOEL を使用することは、げっ歯類の 50%腫瘍発現用量（TD50 等）を使用するよりも保守的である。

Lilly は「医薬品におけるニトロソアミン類の混入リスクに関する自主点検について」（薬生薬審発 1008 第 1 号、薬生安発 1008 第 1 号、薬生監麻発 1008 第 1 号、令和 3 年 10 月 8 日付）に基づき、N-ニトロソアトモキセチンの許容摂取量についての相談を行っている。本資料は当該相談における Lilly の提案とその妥当性について、背景情報を含めてまとめた文書（添付資料）に基づき作成されたものである。

添付資料

- Regulatory Response (Document ID: VV-REG-326326)
- 令和 6 年 7 月 19 日付け電子メールによる照会事項に対する回答書

参考文献

- Sriman De, Bishnu Thapa, Fareed Bhasha Sayyed, Scott A. Frank, Paul D. Cornwell, and Robert A. Jolly, Quantum Mechanical Assessment of Nitrosamine Potency, Chemical Research in Toxicology 2024 37 (6), 1011-1022, DOI: 10.1021/acs.chemrestox.4c00087
- Robert A. Jolly, Paul D. Cornwell, Jessica Noteboom, Fareed Bhasha Sayyed, Bishnu Thapa, Lorrene A. Buckley, Estimation of Acceptable Daily Intake Values based on Modeling and In Vivo Mutagenicity of NDSRIs of Fluoxetine, Duloxetine and Atomoxetine, Regulatory Toxicology and Pharmacology, 2024, 105672, https://doi.org/10.1016/j.yrtph.2024.105672. (https://www.sciencedirect.com/science/article/pii/S0273230024001132)

以上

1. Regulatory Response

LY139603 (atomoxetine)

Japan Ministry of Health, Labour, and Welfare
Date of Questions: 08 August 2024

Eli Lilly and Company

Document ID: VV-REG-326326

2. Introduction/Background

On 08 Augsut 2024, Eli Lilly and Company (Lilly) received a question from the Japan Ministry of Health Labour, and Welfare regarding the proposed AI limit for n-nitroso atomoxetine.

This response answers this question.

3. Questions and Responses

3.1. Question 1

Please summarize the Lilly's opinion including background information and discussion history which assert that 4400 ng/day is safe, scientific, compound-specific and data-based limit for N-Nitroso-atomoxetine or a limit of 1500 ng/day is also reasonable.

3.1.1. Lilly Response to Question 1

Lilly used a weight of evidence method to determine that 4400 ng/day is a safe limit for N-nitroso-atomoxetine. This weight of evidence method used the following to determine the 4400 ng/day limit:

- Known mechanism of action of nitrosamines
- Read-across based on physicochemical properties (Jolly et al 2024)
- In silico models, such as quantum mechanical models (De et al 2024) and QSARFlex (Jolly et al 2024)
- In vivo gene mutation assay (Jolly et al 2024).

For the convenience of the reviewer, the results of the gene mutation assay, which are the primary data supporting a limit of 4400 ng/day, are described below. Results of other supporting data for the limit of 4400 ng/day are provided by literature reference (Jolly et al 2024, De et al 2024).

Importantly, N-nitroso-atomoxetine is clearly differentiated from the more potent nitrosamines in terms of its in vivo mutagenicity and as supported by the read-across analysis. Thus, N-nitroso-atomoxetine does not fall into the Cohort of Concern as identified in ICH M7R2 (2022), which is based on the more potent nitrosamines. ICH M7(R2) has established that the threshold of toxicological concern (TTC) for mutagens that lack carcinogenicity data and that are not in the cohort of concern is 1.5 µg/day (1500 ng/day) chronically for a lifetime. At the TTC, the increase in cancer risk is negligible, which is defined as an excess cancer risk of <1 in 100000 over a lifetime of exposure. On that basis, a limit of 1500 ng/day is scientifically reasonable.

In vivo mutation assay results

N-nitroso-atomoxetine, which was Ames test positive, was tested in an in vivo study of mutagenicity in transgenic rats according to OECD test guidelines and in compliance with GLP requirements. The results demonstrated that N-nitroso-atomoxetine caused an increase in mutant frequency at the *cII* gene in duodenal tissue at a dose level of 100 mg/kg/day and in the liver at dose levels ≥30 mg/kg/day. Mutation frequency was not increased at the lower dose levels of 0.1, 0.537, and 5 mg/kg/day in liver and thus exhibited a "threshold" dose-response relationship. The no-effect-level (NOEL) for in vivo mutagenicity was 5 mg/kg/day and the Benchmark Dose Lower Confidence Limit (BMDL; based on the well-validated benchmark dose approach to data analysis) was 4.4 mg/kg/day. The Acceptable Intake of 4400 ng/d was derived using principles in the ICH M7R2 guidance where the BMDL value was conservatively used in lieu of the TD_{50} value, the dose associated with a 50% tumor incidence (ICH 2023; Note 4).

Lilly believes a mechanism-based risk assessment paradigm for calculation of AI is scientifically justified and warranted in that:

- mutation is a relevant and sensitive endpoint for the assessment of carcinogenic risk of nitrosamines,
- the transgenic rodent model is a robust and well-validated model to assess mutagenicity in vivo.

Further, derivation of the AI using the NOEL or BMDL from the in vivo mutagenicity data is a conservative estimate of risk because:

- the mutagenicity endpoint, as a required precursor to carcinogenicity for nitrosamines, is more conservative than a tumor endpoint,
- use of a dose causing no effects (NOEL) as the point of departure is more conservative than using a dose eliciting a 50% tumor rate in rodents (eg, the TD_{50}).

References

ICH M7(R2) Guideline on assessment and control of DNA reactive (mutagenic) impurities in pharmaceuticals to limit potential carcinogenic risk EMA/CHMP/ICH/83812/2013

Sriman De, Bishnu Thapa, Fareed Bhasha Sayyed, Scott A. Frank, Paul D. Cornwell, and Robert A. Jolly, Quantum Mechanical Assessment of Nitrosamine Potency, Chemical Research in Toxicology 2024 37 (6), 1011-1022, DOI: 10.1021/acs.chemrestox.4c00087

Robert A. Jolly, Paul D. Cornwell, Jessica Noteboom, Fareed Bhasha Sayyed, Bishnu Thapa, Lorrene A. Buckley, Estimation of Acceptable Daily Intake Values based on Modeling and In Vivo Mutagenicity of NDSRIs of Fluoxetine, Duloxetine and Atomoxetine, Regulatory Toxicology and Pharmacology, 2024, 105672,

「ストラテラカプセル及びストラテラ内用液にて検出された新規ニトロソアミンの限度値について」の相談資料に係る
令和 6 年 7 月 19 日付け電子メールによる照会事項に対する回答書

日本イーライリリー株式会社

相談日	品目	内容
令和 4 年 11 月 25 日	ストラテラカプセル5 mg ストラテラカプセル10 mg ストラテラカプセル25 mg ストラテラカプセル40 mg ストラテラ内用液0.4%	新規ニトロソアミンの限度値について

1. 発がん性データのないニトロソアミンについて、Ames 試験とトランスジェニック動物を用いた遺伝子突然変異試験（TGR 試験）が陽性となった場合、現在のガイダンス等では AI を 1500 ng/day より大きい値に設定することを許容しておりません。 N-ニトロソアトモキセチンの TGR 試験における無影響量（NOEL）やベンチマーク用量信頼区間の下限値（BMDL）を発がん試験の NOEL や BMDL と同等に扱っている点は不適切と考えます。 また、TGR 試験結果から直接 AI を算出していますが、ICH M7(R2)ガイドラインでも許容されておりません。（Q&A No. 7.2 参照） したがって、AI の再検討をお願いいたします。

ご照会の件につきまして、以下のように回答いたします。

＜回答＞

日本イーライリリー株式会社及び Eli Lilly and Company（以下、Lilly）は、N-ニトロソアトモキセチンの許容摂取量（AI）は、安全性の観点から、さらに科学的かつ本化合物固有のデータに基づき、4400 ng/day が妥当であると前回の回答と同様に継続して主張する。またそれは現在の規制・ガイダンス、特に ICH M7 Q&A No. 7.2 の記載にも一致していると考えている (Jolly et al. 2024)。上述の ICH M7 Q&A No. 7.2 では、「適切な in vivo 試験の結果は、ケースバイケースでより高い限度値を支持するための、証拠の重み付けに基づく評価に利用可能なデータを補完しうる」と述べている。しかし、Lilly が提出したような in vivo 遺伝子突然変異試験の結果のみにおいて、発がんリスク評価を行うことはできない。Lilly はこれまで回答したように、証拠の重み付けによるアプローチを使用して、4400 ng /day が N-ニトロソアトモキセチンの安全で適切な AI であると判断した。この証拠の重み付けによるアプローチにおいて、Lilly は以下の 4 項目を用いている。

- ニトロソアミン類の既知の作用機序
- 物理的化学的特性に基づくリードアクロス法
- 量子力学モデル (De et al. 2024) 及び QSARFlex 等の In silico モデル
- In vivo 遺伝子突然変異試験

厚生労働省の N-ニトロソアトモキセチンに対する懸念に関して、Lilly は現在の規制・ガイダンスには急速に発展するニトロソアミンリスク評価に関して利用できる科学的知見の全てはまだ反映されていないことを認識している。一方で、Lilly は、N-ニトロソアトモキセチンは強い変異原性を有していない、少なくとも cohort of concern に該当するリスクがあると見なすべきではないことを示す証拠の重み付けアプローチに基づく確固たる論理を展開し提供してきた。ICH M7（R2）では、発がん性データがなく、cohort of concern に含まれない変異原性不純物の毒性学的懸念の閾値（TTC）として、生涯曝露を考慮して 1.5 μg/day（1500 ng/day）を正当化している。当該 TTC においては、発がんリスクは無視できる程度の増加であり、過剰発がんリスクは生涯曝露において 10 万分の 1 未満として定義されている。その考えに基づいて、1500 ng/day を AI として設定することは科学的にも合理的な考え方である。

参考資料

- Sriman De, Bishnu Thapa, Fareed Bhasha Sayyed, Scott A. Frank, Paul D. Cornwell, and Robert A. Jolly, Quantum Mechanical Assessment of Nitrosamine Potency, Chemical Research in Toxicology 2024 37 (6), 1011-1022,
  DOI: 10.1021/acs.chemrestox.4c00087
- Robert A. Jolly, Paul D. Cornwell, Jessica Noteboom, Fareed Bhasha Sayyed, Bishnu Thapa, Lorrene A. Buckley, Estimation of Acceptable Daily Intake Values based on Modeling and In Vivo Mutagenicity of NDSRIs of Fluoxetine, Duloxetine and Atomoxetine, Regulatory Toxicology and Pharmacology, 2024, 105672,
  https://doi.org/10.1016/j.yrtph.2024.105672.
  (https://www.sciencedirect.com/science/article/pii/S0273230024001132)

以上

Chemical Research in Toxicology

pubs.acs.org/crt

Article

Quantum Mechanical Assessment of Nitrosamine Potency

Sriman De, Bishnu Thapa, Fareed Bhasha Sayyed,* Scott A. Frank, Paul D. Cornwell, and Robert A. Jolly*

Cite This: *Chem. Res. Toxicol.* 2024, 37, 1011−1022

Read Online

ACCESS | Metrics & More | Article Recommendations | Supporting Information

ABSTRACT: Nitrosamines are in the cohort of concern (CoC) as determined by regulatory guidance. CoC compounds are considered highly potent carcinogens that need to be limited below the threshold of toxicological concern, 1.5 μg/day. Nitrosamines like NDMA and NDEA require strict control, while novel nitrosamine drug substance-related impurities (NDSRIs) may or may not be characterized as potent carcinogens. A risk assessment based on the structural features of NDSRIs is important in order to predict potency because they lack substance-specific carcinogenicity. Herein, we present a quantum mechanical (QM)-based analysis on structurally diverse sets of nitrosamines to better understand how structure influences the reactivity that could result in carcinogenicity. We describe the potency trend through activation energies corresponding to α-hydroxylation, aldehyde formation, diazonium intermediate formation, reaction with DNA base, and hydrolysis reactions, and other probable metabolic pathways associated with the carcinogenicity of nitrosamines. We evaluated activation energies for selected cases such as *N*-nitroso pyrrolidines, *N*-nitroso piperidines, *N*-nitroso piperazines, *N*-nitroso morpholines, *N*-nitroso thiomorpholine, *N*-methyl nitroso aromatic, fluorine-substituted nitrosamines, and substituted aliphatic nitrosamines. We compare these results to the recent framework of the carcinogenic potency characterization approach (CPCA) proposed by health authorities which is meant to give guidance on acceptable intakes (AI) for NDSRIs lacking substance-specific carcinogenicity data. We show examples where QM modeling and CPCA are aligned and examples where CPCA both underestimates and overestimates the AI. In cases where CPCA predicts high potency for NDSRIs, QM modeling can help better estimate an AI. Our results suggest that a combined mechanistic understanding of α-hydroxylation, aldehyde formation, hydrolysis, and reaction with DNA bases could help identify the structural features that underpin the potency of nitrosamines. We anticipate this work will be a valuable addition to the CPCA and provide a more analytical way to estimate AI for novel NDSRIs.

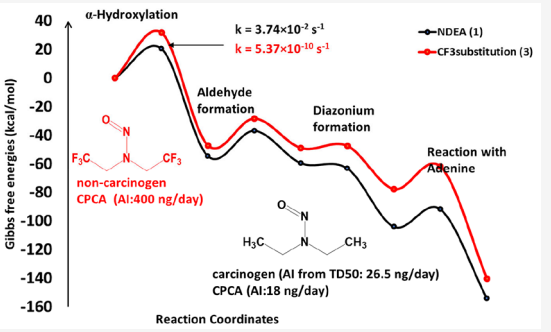

INTRODUCTION

N-nitrosamines are considered part of the cohort of concern (CoC) defined in ICH M7 due to the high carcinogenic potency of the *N*-nitroso structural group[1,2] such that limiting to 1.5 μg/day or the threshold of toxicological concern (TTC), is not considered sufficiently protective and could result in an increase in theoretical cancer risk.[2] Magee and Barnes[3] identified that *N*-nitroso dimethylamine (NDMA) has carcinogenic potential in rats and later studies have shown that most of low molecular weight (LMW) nitrosamines could be carcinogenic.[4−6] In 2018, the US Food and Drug Administration (US FDA) announced a recall of drug products containing valsartan from the market after detecting the presence of NDMA[7] and subsequently, many products have been recalled due to the presence of nitrosamine impurities.[8]

The presence of nitrosamine contaminants in pharmaceuticals led to health authorities including the EMA[9] and FDA[10] to request manufacturers to assess their products for the potential presence of nitrosamines. As these risk assessments were carried out, it became evident that secondary amines in drug substances or related substances had the potential to form complex nitrosamines, referred to as *N*-nitroso drug substance-related impurities (NDSRIs), by reacting with nitrosating agents present during synthesis or in excipients in drug product formulation.[11,12] The EMA and FDA have proposed chronic limits or acceptable intakes (AI) for novel nitrosamines of 18 ng per day and 26.5 ng per day, respectively.[9,10] If an NDSRI is present within a product, then remediation to control its levels to at or below 18 or 26.5 ng/day would be a significant undertaking. That remediation is not guaranteed to be successful or even possible based on the daily dose and physical properties of NDSRIs and excipients in the formulation, which may even preclude analytical detection threshold above these limits. Therefore, efforts to understand

Received: March 4, 2024
Revised: May 6, 2024
Accepted: May 9, 2024
Published: May 28, 2024

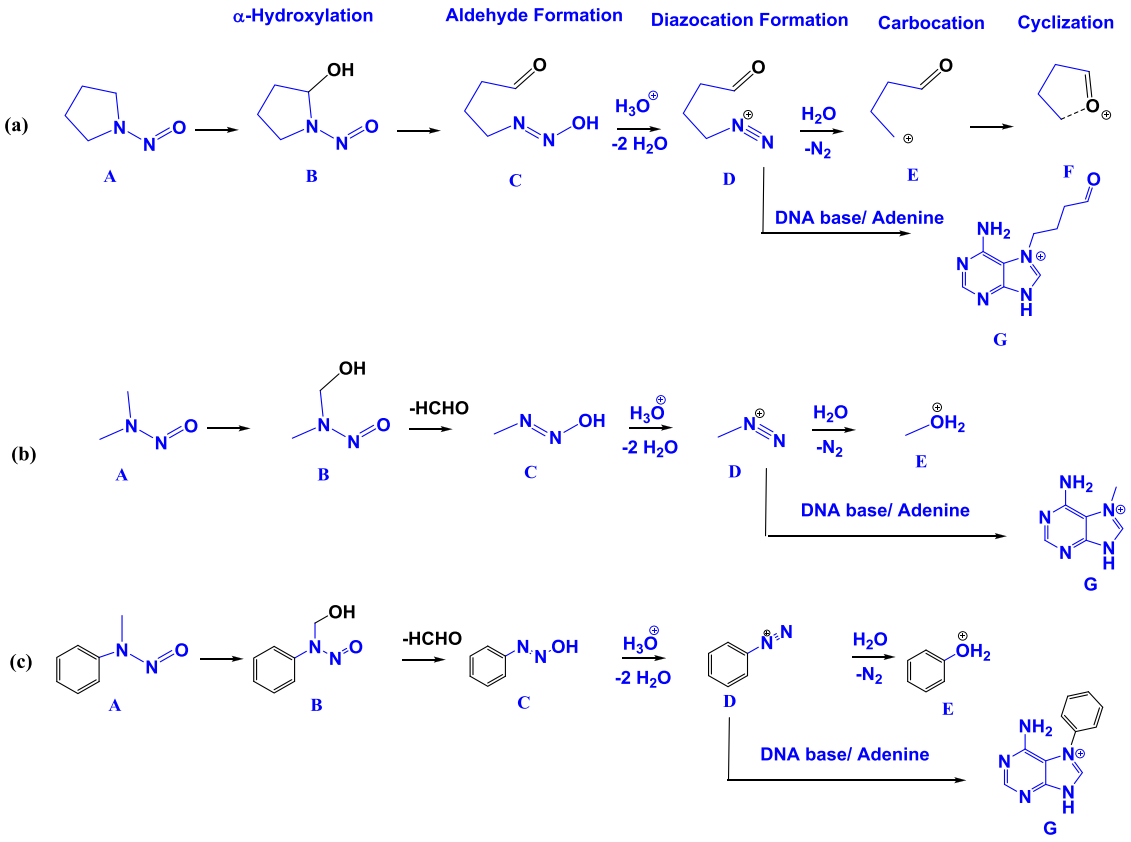

Figure 1. CYP (Cytochrome P450) activated stepwise metabolic pathway for ring, alkyl, and aryl nitrosamines. Carcinogenic metabolic pathway intermediates are labeled as **A**−**G**.

the reactivity of nitrosamines are critical to better estimate AIs for NDSRI compounds.

Experimental data (e.g., rodent carcinogenicity) are not available to support the derivation of a compound-specific AI for most NDSRIs and the defaults of 18 or 26.5 ng/day are highly conservative given that not all *N*-nitrosamines are highly potent carcinogens or even carcinogenic.[13] These default limits for *N*-nitrosamines recommended by agencies are largely based on the TD50 of LMW alkyl *N*-nitrosamines. However, the use of read-through is dependent on the original method of AI derivation. The derivation of the AIs that drive the default values was developed early and many were not derived in a consistent or transparent manner. Bercu et al.[14] showed this recently with a rederivation of AI for several *N*-nitrosamines. By extension, this conservatism in AI derivation magnifies the impact of the analogous AI read across for NDSRIs. Other examples of conservatism in AI derivation include *N*-methyl-*N*-nitrosophenethylamine (NMPEA) and 4-(methylnitrosamino)-1-(3-pyridyl)-1-butanone (NNK)[15] where derived AIs were calculated from pooling organ tumor data while an approach consistent with ICH M7 would result in higher AIs. Perhaps more important is the fact that most NDSRIs are dramatically different from LMW alkyl *N*-nitrosamines based on chemical structure.[16] Differences in physicochemical properties (such as Log P, solubility, polar surface area, etc.), steric hindrance, expected alternate metabolism and clearance pathways, and molecular weight are all expected to dramatically reduce the potential for mutagenic carcinogenicity of NDSRIs.[17,18] In aggregate, these considerations argue that AI derivation has been overly conservative for NDSRIs and that a mechanistic analysis is one area that can be leveraged to improve upon this.

Dobo et al.[18] proposed a framework for the AI limits based on the structure of the nitrosamine. From the common structural features and existing nitrosamine carcinogenic data, they divided nitrosamines into 13 groups and proposed the AI limits conservatively in the range of 17−440 ng/day. Thomas et al.[19] developed three categories of nitrosamine potency nitrosamine potency viz. high potency (TD50 < 0.15 mg/kg/day), medium potency (TD50 in 0.15−1.5 mg/kg/day), and low potency TD50 > 1.5 mg/kg/day). Recently Cross and Ponting[17] reported that the high-potency of nitrosamines is mainly due to α-carbon hydroxylation with those nitrosamines bearing an α-sp^3-hybridized carbon. Steric and electronic effects play a dominant role in the carcinogenic metabolic pathway, and the interplay of these effects can result in a range of potency, from high to low, or even a lack of carcinogenic action. They also reported that electronic withdrawing groups at the α-carbon significantly decrease the potency significantly. Wenzel et al.[20] recently studied the mechanism of aliphatic and cyclic nitrosamines. They showed that hydrolysis and DNA alkylation are competitive, and as the chain length increases the activation energies for the hydroxylation decreases, but DNA alkylation is more favorable thermodynamically. The work of Wenzel et al.[20] gave an understanding of how the structural features affect toxification and detoxification reactions in the nitrosamine metabolic pathway, while the substitution of electron-donating, electron-withdrawing, and presence of heteroatom requires a more detailed understanding.

Nitrosamines require metabolic activation, and the probable carcinogenic metabolic pathway occurs through cytochrome

https://doi.org/10.1021/acs.chemrestox.4c00087
Chem. Res. Toxicol. 2024, 37, 1011−1022

P450 and is shown in Figure 1.[17,18,20,21] The mechanism involves mainly through several steps viz. hydroxylation, aldehyde formation, diazonium cation formation, hydrolysis, or reaction with the DNA base. A detailed mechanistic evaluation of these metabolic steps could help to further develop and generate better AI estimates, and that is the intent of the present work.

Health authorities have proposed guidance that read across and other modeling approaches can be used to determine an AI for NDSRIs.[10] Most recently, agencies have published a carcinogenic potency categorization approach (CPCA) framework to allow manufacturers to generate an AI for NDSRIs.[9,22] The CPCA is fundamentally based on the assumption that nitrosamines are carcinogenic via the α-hydroxylation mechanism. It may be noted that CPCA is applicable to nitrosamines with α-carbon while it is not applicable to *N*-nitrosamides, *N*-nitrosoureas, *N*-nitrosoguanidines, or *N*-nitroso groups, which are part of the aromatic ring.

The CPCA is based on deriving a potency score based on the α-hydrogen count and then adjusting for activating and deactivating features. For Category 1, the AI is 18 ng/day, for Category 2, the AI is 100 ng/day, for Category 3, the AI is 400 ng/day, for Categories 4 and 5, the AI limit is 1500 ng/day. While a reasonable starting framework, the CPCA is largely based on the simple structure read across and the structure−activity relationships described by Cross and Ponting[17] and Dobo[21] and is admittedly overly conservative in its AI determinations. Some estimates indicate that as much as 30 percent of NDSRIs could default to high potency categories 1 and 2.[23] Moreover, when CPCA was used to derive AI nitrosamines against TD50, we observed a few compounds where the AI was overestimated with the majority of AI values being underestimated. In addition, several noncarcinogenic molecules showed up as categories 2 and 3 in CPCA. This underscores the inherent conservatism of the CPCA approach and the need for an additional way to better approximate the AI for NDSRIs in conjunction with the CPCA.

The focus of this work is to determine where clear observations and trends in the mechanistic data can improve AI assessments for NDSRIs. We demonstrate that carcinogenic potency can be rationalized with QM-calculated activation energies for various mechanistic steps involved in the carcinogenic metabolic pathway corresponding to α-hydroxylation, aldehyde formation, diazonium intermediate formation, DNA activation, and hydrolysis reactions in *N*-nitroso pyrrolidines, *N*-nitroso piperidine, *N*-nitroso piperazine, *N*-nitroso morpholine, *N*-nitroso thiomorpholine, *N*-methyl nitroso aromatic, fluorine substituted nitrosamines and substituted aliphatic nitrosamines. In the present work, we consider molecules only with α-sp^3 hybridized carbon on at least one side of the *N*-nitroso group.

COMPUTATIONAL DETAILS AND METHODOLOGY

All the computational calculations have been performed with Gaussian 16 suite programs.[24] All the structures are optimized with B3LYP method with empirical dispersion correction (D3BJ)[25] and 6-31+G(d,p) level of theory.[26,27] As a model compound for the P450 oxidant, the truncated porphyrin Fe-complex (represented as **cpd1**) shown in Figure 2 is considered. Previous reports suggested this model accurately represents the P450 oxidant mechanism.[28] The geometry optimization as well as the transition state (TS) structures involved with **cpd1** were performed with the B3LYP/BS1

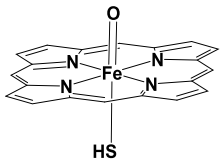

Figure 2. Model compound for P450 oxidation (**cpd1**).

method (BS1: C, H, N, O, S, F-6-31G(d) and Fe-LANL2DZ) method with water as solvent employing SMD model.[29,30] Further, single-point calculations were performed on the Fe-complexes at the B3LYP-D3BJ/BS-II level (BS-II: C, H, N, O, S, F-6-31+G(d, p), and Fe-SDD). Based on the literature,[28] data for the nitrosamine reactions involved with **cpd1**, the high spin state was considered for molecules with alkyl/substituted alkyl systems, and both low spin as well high spin were considered for aromatic systems (Supporting Information). The infrared (IR) frequency calculations were performed on all the optimized geometries to verify the minima and the first-order saddle points. Transition state structures were verified with one imaginary frequency (NIMAG = 1) connecting reactants and products and no imaginary frequencies for the reactants, intermediates, and products (NIMAG = 0). The rate constants are calculated using the below equation where k_B is the Boltzmann constant and h is Planck's constant.[31]

$$k = \frac{k_B T}{h} e^{-\Delta G^{\ddagger}/RT}$$

Throughout this article, Gibbs free energies are used for discussion. In Figure 1, nitrosamine metabolic pathway intermediates are labeled as **A**, **B**, **C**, **D**, **E**, **F**, and **G**. The same notation was adopted to represent the Gibbs free energies. For instance, $\Delta G^{\ddagger}_{AB}$ represents the free energy of activation for the α-hydroxylation reaction of **A** with **cpd1**. $\Delta G^{\ddagger}_{BC}$ represents the activation barrier for the aldehyde formation step. $\Delta G^{\ddagger}_{DE}$ and $\Delta G^{\ddagger}_{DG}$ represent the free energy of activation for hydrolysis and reaction with DNA base, respectively. We considered adenine as a representative of the DNA base to understand the reactivity of nitrosamines for DNA alkylation.

Data Set. The data set for this study was curated from the Lhasa Carcinogenicity Database (LCDB, carcdb.lhasalimited.org).[13] From the available nitrosamines, only the secondary nitrosamines (i.e., C−N(N=O)−C substructure) were selected for further analysis. We excluded other classes of compounds containing non-hydrogen heteroatoms at the α position of the nitrosamine or carbonyl group such as nitrosamide, nitrosacarbamate, nitrosourea, and other similar classes that are known to be potentially mutagenic and/or carcinogenic via different mechanisms. Additionally, compounds containing multiple nitroso groups were excluded from the analysis. For the quantitative analysis related to the TD50, the original TD50 values calculated by Gold et al. (herein referred to as TD50) are used as a primary experimental reference and the values derived by Lhasa Limited (herein referred to as Lhasa TD50) are referenced as needed (both available in LCDB). We selected only the molecules with rodent in vivo data to avoid the discrepancy in data from different species (discussed later in the Results and Discussion section). Note that even within the data sets for rodents, there is still some discrepancy (male versus female, two-dose range versus multiple-dose range; tumour type, etc.). We considered TD50 values from the work of Thomas et al.[19] The common

https://doi.org/10.1021/acs.chemrestox.4c00087
Chem. Res. Toxicol. 2024, 37, 1011−1022

structures considered in the present study are classified into three broad classes, alkyl, aryl, and alicyclic nitrosamines as shown in Figure 3.

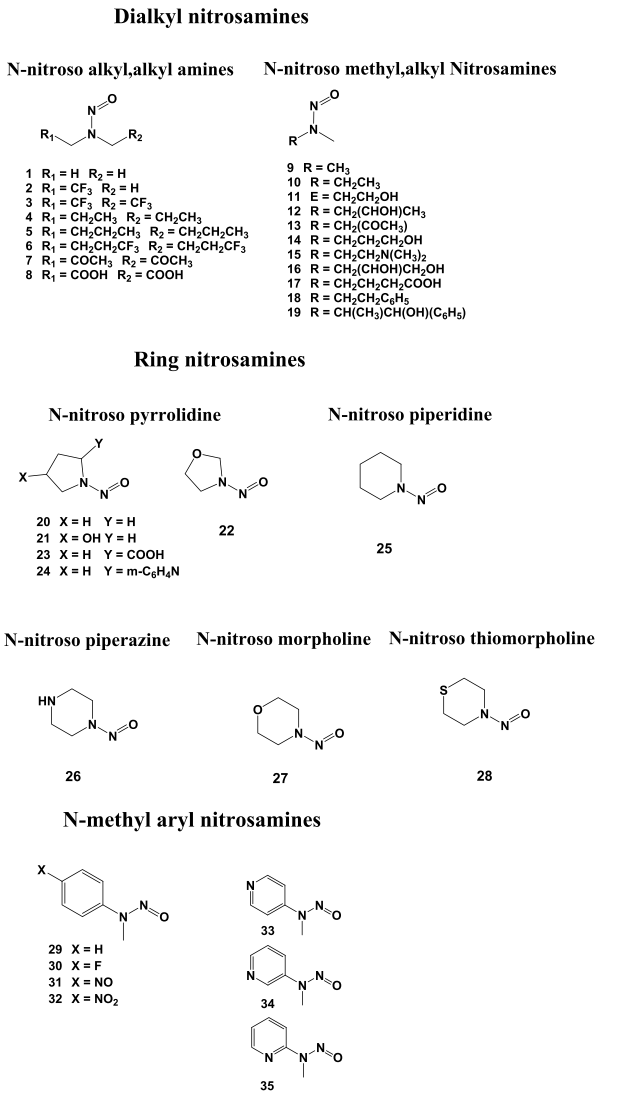

Figure 3. Nitrosamines considered in the present work.

This classification is primarily based on the assumption that the fundamental chemical subunits that are unique in terms of reactivity can be derived from the complex nitrosamines, and the effect of structural complexity on TD50 can be rationalized and understood using the appropriate tools (a "bottom-up" approach). For the subclass formation, we focus on the reactivity of hydrogens on the carbon next to the nitroso group (α-hydrogen atoms) within each subclass which has been established to be the key step in the metabolic cascade of nitrosamines.[17] With this classification, we aim to show that the effect of various substituents (i.e., electronic and steric effects) on a particular subclass can be satisfactorily described through careful modeling of reactivity using quantum mechanics. For the brevity of the manuscript, we have focused our discussion on some specific subclasses where diversity in the molecules and dynamic range of the TD50s are available (vide infra). A similar analysis could be expanded to the whole nitrosamine data set. Furthermore, this approach is consistent with the underpinnings of the CPCA framework in recent guidance on nitrosamine AI limits but provides the structural basis of the reactivity beyond the predefined substructure-based classes to determine individual AI substance-specific limits.

RESULTS AND DISCUSSION

We utilized the quantum mechanical activation energies corresponding to α-hydroxylation, aldehyde formation, diazonium intermediate formation, DNA activation, and hydrolysis reactions to understand the carcinogenic potency trends. In particular, the discussion is focused on the selected series of compounds such as *N*-nitroso pyrrolidines, *N*-nitroso piperidine, *N*-nitroso piperazine, *N*-nitroso morpholine, *N*-nitroso thiomorpholine, *N*-nitroso *N*-methyl aromatic, fluorine substituted nitrosamines, and substituted aliphatic nitrosamines for which significant experimental data is available to rationalize the trends.

Substituent Effect in Dialkyl-Substituted Nitrosamines. Figure 4 represents nitrosamines with electron-donating substitution methyl (**1**), ethyl (**4**), propyl (**5**), and electron-withdrawing CF_3 (**2**, **3**, **6**), $COCH_3$ (**7**), and COOH (**8**) substitutions at α-carbon. Compounds **3** and **8** are noncarcinogenic and are included in this study to compare the

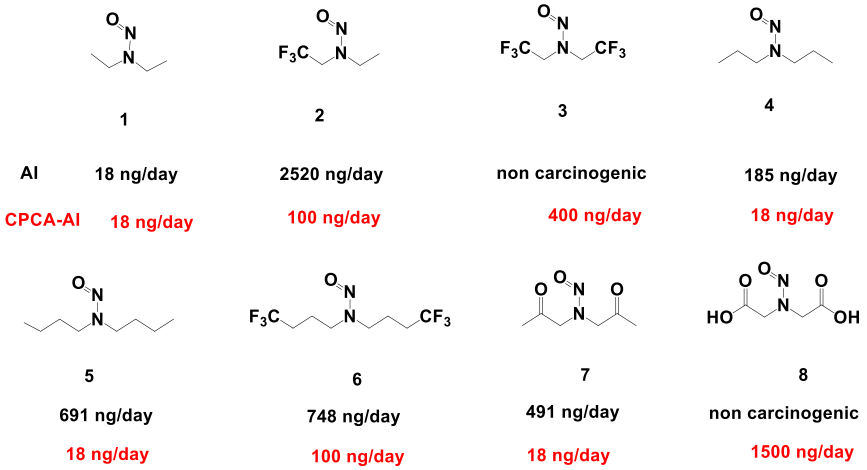

Figure 4. Nitrosamines illustrating electron withdrawing and electron donating substituent effects along with AI values based on TD50 values.[19] The red color values show predicted AI values from the CPCA score.

https://doi.org/10.1021/acs.chemrestox.4c00087
Chem. Res. Toxicol. 2024, 37, 1011−1022

reactivity of noncarcinogens with carcinogenic nitrosamines assuming that all the compounds undergo α-hydroxylation. We reiterate the fact that the −COOH group is considered to be only a substituent to understand the electron-withdrawing effect. The AI values range from 70 ng/day (**1**) to 2520 ng/day (**2**)[19] which covers five categories described to predict AI through the CPCA approach from the regulatory (in the range of 18−1500 ng/day).[2,9] As shown in Figure 4, for all of these molecules, CPCA significantly underestimates the AI values. For molecules like **1** (NDEA) and **8** the predicted AI is reasonable while for noncarcinogenic compound **3**, the predicted AI is 400 ng/day. QM modeling of the metabolic pathway for these molecules was used to understand the differences between noncarcinogens and carcinogens as per the mechanism shown in Figure 1b.

In Table 1, the Gibbs activation energies for the nitrosamine metabolic pathway for compounds **1**−**8** are reported. The

Table 1. Gibbs Free Energies of Activation (kcal/mol) of Compounds 1−8 for the Nitrosamine Metabolic Activation Mechanism

nitrosamine	$\Delta G^{\ddagger}_{AB}$	$\Delta G^{\ddagger}_{BC}$	$\Delta G^{\ddagger}_{DE}$	$\Delta G^{\ddagger}_{DG}$
1	19.4	17.8	12.1	12.2
2	19.6	21.4	18.1	15.9
3	30.7	18.8	18.1	15.9
4	17.0	18.0	12.0	11.2
5	16.4	17.1	11.7	10.7
6	17.6	17.2	12.4	14.3
7	17.1	20.8	19.3	16.3
8	20.1	23.4	16.3	14.2

$\Delta G^{\ddagger}_{AB}$ of the α-hydroxylation step is in the range of 17.0−30.7 kcal/mol. The lowest $\Delta G^{\ddagger}_{AB}$ (17.0 kcal/mol) is observed for compound **5** which has an electron-donating butyl group, indicating that the α-hydroxylation process is kinetically favored. Similarly, compounds with electron-donating substituents on both sides of the nitrosamine group are in the range of 16.4 (**5**)−19.4 (**1**) kcal/mol. The calculated rate constant, $k = 5.37 \times 10^{-10}$ s^{-1}, for molecule **3** is almost negligible when compared to the rate of α-hydroxylation for NDEA or compound **1** ($k = 3.74 \times 10^{-2}$ s^{-1}). Therefore, based on the k_{OH} values the molecule can be assigned to a lower potency or noncarcinogenic category. It may be noted that health authorities guidelines for the CPCA approach are also based on the assumption that nitrosamine molecules undergo the α-hydroxylation process.[9] Interestingly, compounds with carbonyl substitution, which has a tendency for electron delocalization, also showed lower $\Delta G^{\ddagger}_{AB}$ values compared to those of the alkyl substitution. This suggests that the presence of electron-withdrawing groups on α-carbon on both sides of the nitroso group may not necessarily lead to a noncarcinogenic nature or lower potency, but rather it is highly dependent on the type of electron-withdrawing substituent. In this regard, Thomas et al.[19] also recently reported that the presence of β-carbonyl groups can increase potency and quantum mechanical calculations corroborated the observation.

Further, $\Delta G^{\ddagger}_{AB}$ for compound **6** is 17.6 kcal/mol wherein the electron-withdrawing CF_3 group attached to γ-carbon is very close to the $\Delta G^{\ddagger}_{AB}$ of compound **4** indicating that electron-withdrawing substitution further away from α-carbon exerts a diminished effect on the α-hydroxylation process. The calculated rate constants for compounds **4** and **6** are 2.15 and 0.78 s^{-1}, respectively. Thus, for the α-hydroxylation process, the presence of electron-withdrawing groups like CF_3 (non-carbonyl) at α-carbon decreases the potency while the presence of electron-donating alkyl groups is likely to have higher potency. Based on results analyzed in this series, and in general, the presence of strong electron-withdrawing groups like CF_3 can significantly affect the alpha hydroxylation and in turn increase the observed AI values calculated from TD50. While the QM modeling is generally in line with the CPCA on electron-withdrawing groups being deactivating groups toward potency, our data suggest that the extent of α-hydroxylation activation/deactivation can depend on the strength of the electron-withdrawing group resulting in a variable effect and should be accounted separately (CPCA considers all EW groups to be equivalent with carbonyl as an exception).

The next step in the mechanism is the elimination of the aldehyde by the proton transfer reaction of OH to the nitrosamine group. The reaction free energies ΔG_{BC} for **1**−**8** are in the range of −46.0 to −62.1 kcal/mol, **1**, **2**, **4**, **5**, and **6** exothermic relative to the precursor intermediate while **2** and **7** are endothermic (Supporting Information Table S1). Furthermore, the $\Delta G^{\ddagger}_{BC}$ for this process is higher for electron-withdrawing substituents at α-carbon to the nitrosamine group when compared to the electron-donating compounds **1**, **4**, **5**, and **6**. The last step is the competitive pathways for the hydrolysis or the reaction with a DNA base. For both hydrolysis and DNA base reactions, electron withdrawing compounds **2**, **3**, and **7** had a higher activation energy than the electron donating substituted **1**, **4**, **5**, and **6**. This suggests that electron-donating diazonium is relatively more reactive than electron-withdrawing substituted diazonium molecules.

In Figure 5, the comparison of Gibbs free energy profiles between the most potent carcinogenic nitrosamine NDEA (**1**)

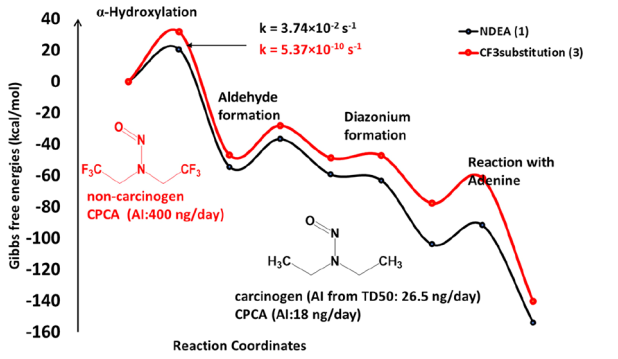

Figure 5. Comparison of Gibbs free energy profiles between NDEA (**1**) and CF_3 substituted nitrosamine **3**. **1** (NDEA) is the most potent carcinogen while **3** is noncarcinogenic compound. Data points are Gibbs free energies in kcal/mol.

and noncarcinogenic compound **3** clearly shows that carcinogenic nitrosamine metabolic pathway has a lower free energy profile and noncarcinogenic molecules occur through a higher energy profile. From the above discussion, in the case of compounds **1**-**8**, overall mechanistic understanding is crucial for the assessment of nitrosamine potency, as evident from the quantum mechanical data.

Taken together, these data show that an EWG is species and location-dependent, and QM modeling illustrates and models the importance of such effects. These insights can be used for

https://doi.org/10.1021/acs.chemrestox.4c00087
Chem. Res. Toxicol. 2024, 37, 1011−1022

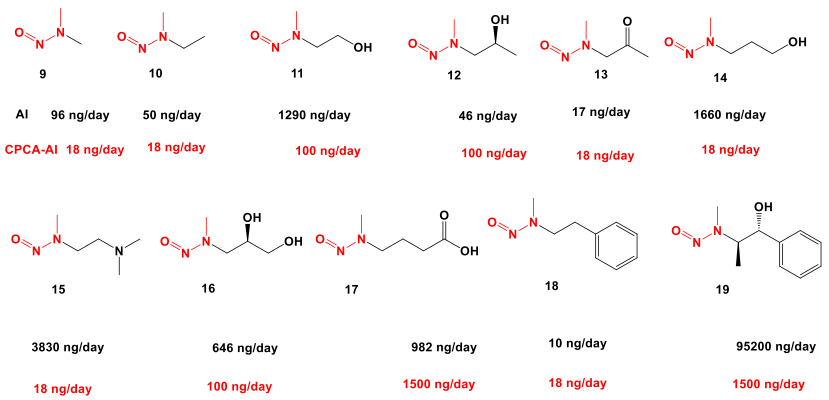

Figure 6. *N*-methyl nitroso substituted alkyl compounds considered in the present study. The AI values from TD50s as well as the predicted CPCA AI values (in red) are shown.

Table 2. Gibbs Free Energy of Activation (in kcal/mol) for the Mechanistic Steps Involved in the *N*-methylalkyl Series

nitrosamine	$\Delta G^{\ddagger}_{AB}$	$\Delta G^{\ddagger}_{AB}{}'$	$\Delta G^{\ddagger}_{BC}$	$\Delta G^{\ddagger}_{BC}{}'$	$\Delta G^{\ddagger}_{DE}$	$\Delta G^{\ddagger}_{DG}$	k_α'/k_α [a]
9	21.6	21.6	23.1	23.1	15.3	13.2	1.0 [b]
10	21.7	19.6	22.3	18.5	12.1	12.2	34.6
11	21.2	19.8	22.5	19.4	13.3	12.8	10.6
12	20.6	21.2	24.7	18.2	14.5	13.4	0.4
13	18.4	17.3	22.3	20.7	19.3	16.3	6.4
14	21.6	19.6	22.5	18.7	12.4	11.5	29.2
15	20.9	19.0	22.8	19.3	11.7	11.9	24.7
16	20.1	18.9	22.1	18.7	14.1	12.2	7.6
17	21.6	18.6	23.5	18.7	11.5	10.0	158.1
18	20.5	18.4	22.9	19.0	11.6	11.3	34.6
19	19.9	20.2	23.0	12.1	12.5	12.9	0.6

[a]Ratio of rate constants k_α' and k_α calculated from $\Delta G^{\ddagger}_{AB}$ and $\Delta G^{\ddagger}_{AB}{}'$, respectively. [b]NDMA (9) has same alkyl groups on both sides of N-NO group, so the k_α'/k_α is 1. When hydroxylation occurs at the alkyl side of the nitrosamines 9−19, $\Delta G^{\ddagger}_{DE}$ and $\Delta G^{\ddagger}_{DG}$ will remain same as for the molecule 9.

WOE arguments on potency and nitrosamines supporting AI determination.

***N*-methylalkylnitrosamines.** Figure 6 shows the *N*-methyl nitrosoalkylamines (compounds **9**−**19**). All these nitrosamines have a CH_3 group on one side of the *N*-nitroso moiety and a substituted alkyl group with two α-hydrogens on the other side. As α-hydrogens are present on both sides, α-hydroxylation can occur on either side. These molecules cover β-hydroxy substitution, carbonyl, electron-donating NMe_2, and benzyl and hydroxy-substituted benzyl groups with an AI in the range of 10−95,200 ng/day.

We performed QM calculations on the carcinogenic metabolic pathway (Figure 1b) to understand the potency trends for these compounds. The activation energies for both sides of the C−H bonds (Table 2) are evaluated, $\Delta G^{\ddagger}_{AB}$ and $\Delta G^{\ddagger}_{AB}{}'$ represent α-hydroxylation activation energy for the *N*-methyl group and CH_2 of the more substituted alkyl side, respectively. $\Delta G^{\ddagger}_{AB}$ is in the range of 18.4−21.7 kcal/mol whereas $\Delta G^{\ddagger}_{AB}{}'$ 17.3−21.6 kcal/mol and the ratio of calculated rate constants from the k_α'/k is 0.4 to 158 orders of magnitude suggesting that α-hydroxylation can occur on both α−C-H bonds but are kinetically preferable on the more substituted alkyl side for a majority of the nitrosamines shown in Figure 6. Compound **9** is NDMA, with $\Delta G^{\ddagger}_{AB}{}'$ being 21.6 kcal/mol, while for compound **10**, it is 19.6 kcal/mol which is lower because of the alkyl CH_3 group substitution which provides additional stabilization to radical formed during C−H activation.[32] $\Delta G^{\ddagger}_{AB}{}'$ for compound **11** is 19.8 kcal/mol which is comparable to the **10** indicating that OH substitution at β-carbon shows a minor influence on the α-hydroxylation process.

Interestingly, $\Delta G^{\ddagger}_{AB}{}'$ for compound **12** is 21.2 kcal/mol which is an increase of 1.4 kcal/mol from compound **11** and which indicates that when double substitution is present at β-carbon, stereo electronic effects play a crucial role in the hydroxylation process. Furthermore, the $\Delta G^{\ddagger}_{AB}$ for compound **12** is 20.6 kcal/mol which is slightly lower than $\Delta G^{\ddagger}_{AB}{}'$ which would be a kinetically preferable site. However, compound **12** also has a secondary alcoholic group (AI is 46 ng/day) and is a much more potent carcinogen compared to compound **11** (AI is 1290 ng/day). Interestingly, compound **11**, which has a primary alcoholic group, can undergo alcohol oxidation to aldehyde instead of α-hydroxylation at C−H site whereas compound **12** is likely to undergo α-hydroxylation. Recently, Snodin et al. reported that compounds with primary as well as secondary hydroxy groups undergo competitive phase I and/or phase II metabolic pathways (Sulfation, glucuronidation and primary oxidation). Further, in the case of β-hydroxy compounds, the increased potency is expected because of alternative ways of forming alkyl diazonium ions.[36b] This could be a potential reason for a significant difference in potency between **11** and **12** (the effect of alternative metabolic pathways is not included in this study).[33,34] Compound **13** has the lowest $\Delta G^{\ddagger}_{AB}{}'$ of 17.3 kcal/mol and also a very low AI of 17 ng/day which could be because of the extended conjugation provided by the carbonyl substitution at the α-carbon. Thomas

https://doi.org/10.1021/acs.chemrestox.4c00087
Chem. Res. Toxicol. 2024, 37, 1011−1022

et al.[19] reported that β-carbonyl substitution increases the potency. The QM calculations illustrate that α-hydroxylation is easier if the nitrosamine has a β-carbonyl substitution.

The CPCA-derived potency score for the molecules **9**−**19** is simply the α-hydrogen score, which is 1 (3 hydrogens on one side and 2 hydrogens on the other) and falls under the category 1 corresponding to 18 ng/day. Molecules **11**, **12**, **16**, and **19** all have a β-hydroxy group as the deactivating structural feature with a potency score of 2 and therefore fall under category 2 with a 100 ng/day AI limit. For these molecules, the CPCA category mostly underestimates the AI range calculated from the actual TD50. However, molecule **17** falls under category 4 corresponding to a 1500 ng/day AI limit (actual AI is 982 ng/day). This is an example where CPCA overestimates the potency.

The molecule **15** has a β-substituted $N(CH_3)_2$ group with AI of 3830 ng/day, and CPCA predicted AI is 18 ng/day. For this molecule, possible alternate hydroxylation mechanisms via dealkylation or oxygenation were also considered and are shown in Figure 7. The calculated activation energy for the *N*-

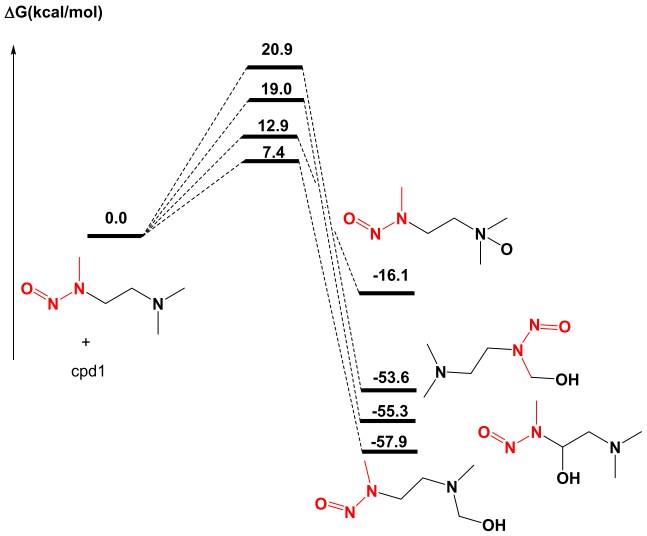

Figure 7. Probable competitive pathways α-hydroxylation, *N*-dealkylation and *N*-oxygenation of **15** by **cpd1**. Gibbs activation free energies represent that α-hydroxylation is not the preferred pathway, despite having two CH_2 groups at the α-position.

dealkylation is 7.4 kcal/mol and for *N*-oxygenation is 12.9 kcal/mol, which is substantially lower than α-hydroxylation (19.0 kcal/mol).[35] It indicates that compound **15** can undergo other competitive metabolic mechanisms, and hence, the carcinogenic mechanism is kinetically least preferred. Thus, the variation observed in the AI also can strongly depend on the potential of undergoing alternate metabolism, and that needs to be carefully considered while assessing the AI limits for NDSRIs. Overall, the discussion above further shows that the QM calculations can be used as a viable tool to further evaluate and adjust the AI limits for NDSRI compounds where CPCA falls short.

The AI values for compounds **9**, **10**, **12**, **13**, and **18** are 96, 50, 46, 17, and 10 ng/day, respectively which supports the fact that nitrosamines with *N*-methyl and *N*-alkyl combination with α−C-H in the alkyl group have low AI when compared to doubly substituted compounds such as **16** and **19** (AI is 646 and 95,200 ng/day, respectively). To further confirm the trend of observed α-hydroxylation ($\Delta G^{\ddagger}_{AB}{}' > \Delta G^{\ddagger}_{AB}$), we performed transition state structure calculations (TSBC) for the proton transfer mechanism on both sides of α-hydroxylated molecules. The aldehyde formation step is endergonic relative to the hydroxylation step for the ΔG_{BC} when compared with $\Delta G_{BC}{}'$ (Supporting Information). The activation energies for the aldehyde formation step follow a similar trend $\Delta G^{\ddagger}_{BC} > \Delta G^{\ddagger}_{BC}{}'$ which further confirms that alkyl aldehyde formation is preferred both kinetically as well as thermodynamically (Table S1). Wenzel et al.[20] also found a similar observation that methyl group elimination had a high activation energy and endergonic in the case of *N*-methyl, long-chain nitrosamines. Therefore, from the above discussion, for all molecules **9**−**19**, the methyl diazonium intermediate or the corresponding alkyl diazonium intermediate can be formed. The activation energies for the hydrolysis and DNA base are reported in Table 2. Overall, the quantum mechanical data provide a further reactivity-based explanation to the experimentally observed potency trends of *N*-methyl nitrosamines. This further suggests that the CPCA scoring and classification can be augmented with QM analysis to understand and give a better AI estimation for NDSRIs.

Ring Nitrosamines. *N-Nitroso Pyrrolidines.* Substituted *N*-nitroso pyrrolidine compounds (**20**−**24**) are shown in Figure 8. In this class of molecules, a nitroso group is attached

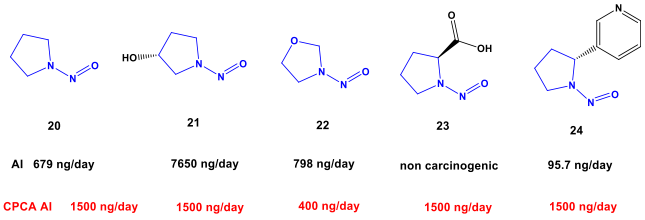

Figure 8. *N*-nitroso pyrrolidine compounds. AI from TD50 and CPCA predicted AI limits is also shown.

to an amine nitrogen which is a part of a five-membered ring. These compounds represent the effect of OH substitution (**21**), the presence of heteroatom which is part of the ring (**22**), electron-withdrawing COOH (**23**), and aromatic substitution, NNN (**24**). In the CPCA, this class of molecules has a deactivating feature score of +3 which would be expected to have low potency because of the high CPCA score. The TD50 values for these molecules range from 0.0957 to 7.65 mg/kg/day. The highest potency is observed for a *m*-pyridine substituted at the α-position *N*-nitroso pyrrolidone (NNN, **24;** 0.0957 mg/kg/day). For **20**−**24,** we evaluated the reaction energy profiles for all the metabolic steps involved in the carcinogenic metabolic pathway shown in Figure 1a. The $\Delta G^{\ddagger}_{AB}$ is in a narrow range of 18.4−20.3 kcal/mol (rate constants are in the range of 2.4×10^{-1}−8.2×10^{-3} s^{-1}). The relative rate constants of α-hydroxylation with respect to compound **20** are 0.18, 4.57, 4.57, and 2.75-fold. Figure 9 shows the optimized transition state geometries for compounds **20**−**24**. The geometrical data are very similar in compounds **20**−**24** and the C−H bond distances are in the range of 1.307−1.323 Å and the O−H bond distances are in the range of 1.217−1.240 Å showing no significant changes (Table 3). These data indicate that probably the other steps in this metabolic pathway could be playing a rate-limiting role in such variation as discussed below.

https://doi.org/10.1021/acs.chemrestox.4c00087
Chem. Res. Toxicol. 2024, 37, 1011−1022

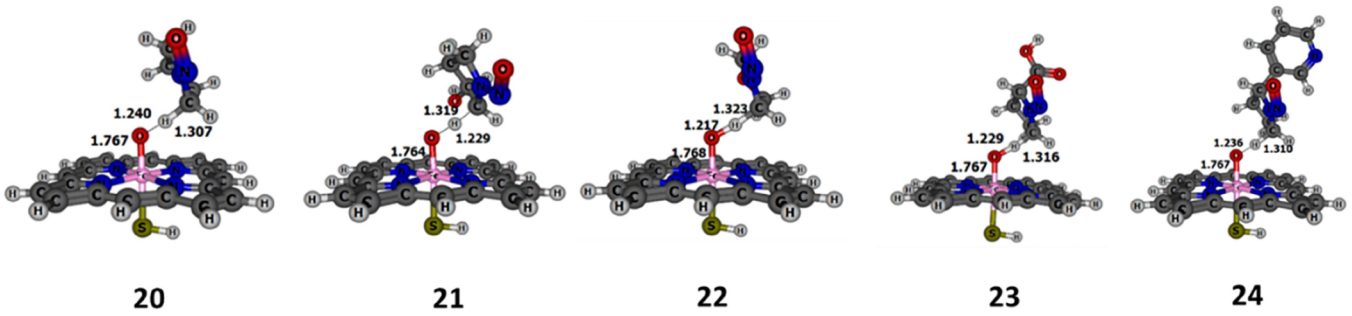

Figure 9. Optimized transition state geometries of compounds **20-24**. All the bond lengths are shown in Å.

Table 3. Gibbs Activation Free Energies (kcal/mol) for Various Mechanistic Steps for Compounds 20−24

	20	21	22	23	24
$\Delta G^{\ddagger}_{AB}$	19.4	18.4	20.3	20.3	20.0
$\Delta G^{\ddagger}_{BC}$	22.1	21.8	18.8	23.6	22.6
$\Delta G^{\ddagger}_{DE}$	13.5	15.7	13.5	12.1	6.9
$\Delta G^{\ddagger}_{DG}$	14.4	16.6	13.3	13.3	4.0

The second step in the metabolic pathway is the aldehyde formation (Figure 1a) due to hydrogen transfer from the α-hydroxyl group to the nitrosamine group as shown in Figure 10. The $\Delta G^{\ddagger}_{BC}$ values are higher than the $\Delta G^{\ddagger}_{AB}$ except for

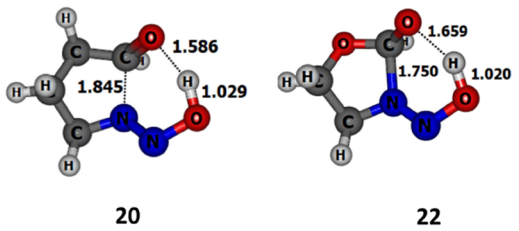

Figure 10. Aldehyde formation step transition state structures of compounds **20** and **22**. All of the bond lengths are shown in Å.

compound **22** (*N*-nitroso oxazolidine) which suggests that the rate-determining step is the ring opening of five-membered pyrrolidine affording to the aldehyde. This compound formed after the ring opening, can further undergo deactivating metabolism or oxidation to acids which can be glucuronidated, and in general, phase 2 metabolism should be considered. This compound formed after the ring opening, can be further undergo deactivating metabolism or oxidation to acids which can be glucuronidated, and in general, phase 2 metabolism should be considered.[36b] In case of compound **22**, the rate-determining step is α-hydroxylation. To explain the reactivity differences between pyrrolidine and oxazolidine nitrosamines, the transition state geometries are observed. The transition state geometries of the ring-opening reaction showed a clear difference. The C−N bond distance in TSBC of **22** is 1.750 Å while it is 1.845 Å in **20** which could be potentially due to the reduced ring strain in **22**.[36] The calculated reaction-free energies for **22** are also thermodynamically more favorable than other *N*-nitroso pyrrolidines (Table S1). This is most likely due to the formation of formate in **22** after ring opening whereas in other molecules ring opening leads to the formation of aldehydes.

The next step in the metabolic pathway is the diazonium cation formation via the elimination of the hydroxyl group from the N═NOH group, and this process is highly exothermic. As discussed before, the diazonium cation will have competing reactions with DNA bases or reaction water, which is also one of the factors that could influence the mutagenic potential of nitrosamines. For this series, the hydrolysis and DNA base adenine reaction are found to be competitive as the difference between activation energies is in the range of 0.9−1.2 kcal/mol. It should be noted that compound **23** is noncarcinogenic as it may undergo phase II metabolic pathway related to the carboxylic acid group and, in this study, we show how the electron withdrawing group can influence the overall nitrosamine metabolic pathway.

In the previous section, we showed that CPCA underestimates the AI for compound **15**, and herein, we showed an example that AI is overestimated for compound **24**. Within compound series **20**−**24**, the α-hydroxylation process is not the only parameter that can define the trend in the TD50. In the CPCA, the nitroso group which is part of the five-membered ring gets a higher deactivating score than the corresponding six-membered ring. The predicted CPCA-AI for *N*-nitroso pyrrolidine is 400 ng/day, which is quite reasonable when compared with the actual 679 ng/day so that it conservatively defines the limit for NDSRIs that would have nitroso pyrrolidines. However, *N*-nitroso pyrrolidine series, shows examples wherein predicted CPCA-AI overestimates and/or underestimates than the actual AI. Notably, molecule **24** predicted AI is 1500 ng/day but the actual AI is 95.2 ng/day.

For compound **24**, Ma et al.[28] recently studied the probable metabolic pathways which are summarized in Figure 11 showing the potential toxifying and detoxifying pathways. Among all of the possible reactivity sites, α-hydroxylation is the most preferred pathway for NNN (**24**). Though CPCA predicts 1500 ng/day AI for this compound because of the preferred carcinogenic metabolic pathway actual AI is only 95.7 ng/day. This is one more example wherein QM calculations emphasize the importance of understanding the nitrosamine reactivity and help in addressing AI limits for NDSRIs. Additionally, Thomas and coworkers[19] suggested that molecules with multiple sets of structural features can undergo various metabolic pathways that require additional expertise and analysis to understand the potency trend, and QM calculations could be useful to understand and justify the AI limits.

Heteroatom Effect on Six-Membered Saturated Rings wherein N-NO Is Part of the Ring. In this section, we explored the reactivity of molecules wherein the nitrosamine is part of the six-membered saturated ring with a heteroatom part of the ring system. We selected four molecules, namely, *N*-nitroso piperidine (**25**), *N*-nitroso piperazine (**26**), *N*-nitroso morpholine (**27**), and *N*-nitroso thiomorpholine (**28**) shown

https://doi.org/10.1021/acs.chemrestox.4c00087
Chem. Res. Toxicol. 2024, 37, 1011−1022

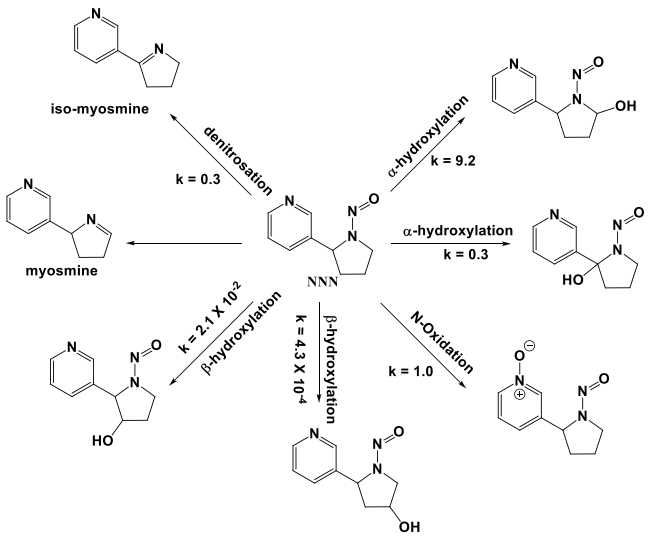

Figure 11. Possible metabolic pathways of NNN. Rate constants (s-1) predicted from QM calculations are taken from reference Ma et al.[28]

Table 4. Gibbs Activation Free Energies for All the Mechanistic Steps or the Compounds 25, 26, 27, and 28

nitrosamine	$\Delta G^{\ddagger}_{AB}$	$\Delta G^{\ddagger}_{BC}$	$\Delta G^{\ddagger}_{DE}$	$\Delta G^{\ddagger}_{DG}$
25	19.9	16.0	11.9	12.0
26	19.3	16.4	11.4	13.1
27	19.7	16.5	13.5	12.0
28	20.2	14.9	13.3	12.3

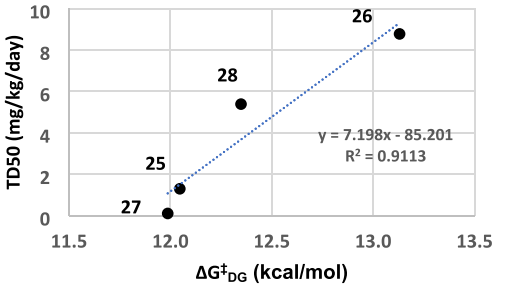

Figure 13. Correlation between Gibbs activation free energies of reaction with the DNA base.

in Figure 12. These four compounds differ by the substitution of a heteroatom in the ring system at the fourth position. The TD50 values are 1.30, 8.78, 0.109, and 5.39 mg/kg/day for compounds **25**, **26**, **27**, and **28**, respectively. This indicates that piperazine has low potency, while morpholine has the highest potency among the four. In the CPCA scoring, both EMA[9] and FDA[22] reported that deactivating feature score for **25**−**28** follows the order **28** (+3) > **26**(+2) = **25**(+2) > **27**(+1). The activation energies for α-hydroxylation of all these four compounds are in the narrow range of 19.3−20.2 kcal/mol (k = 4.43 × 10^{-2} s^{-1} to k = 9.69 × 10^{-3} s^{-1}), showing no significant variation to explain the heteroatom effect, Table 4. However, for the aldehyde formation step, S-containing **28** showed a considerably lower activation energy of 14.9 kcal/mol when compared to compounds **25**, **26**, and **27**. In the case of hydrolysis, compounds **25** and **26** both have low activation energies and in the case of reaction with DNA base adenine, **26** has the highest activation energy which is consistent with the TD50 values.

A correlation between TD50 and $\Delta G^{\ddagger}_{DG}$ (Figure 13) was observed within a 6-membered ring series. This correlation can be used to understand the scientific rationale for the reactivity of the NDSRIs with heteroatom. It may be noted that molecules **26** and **28** have higher TD50 than others in the series and this could be further explained by considering competitive metabolic pathways. In Figure 14a, the probable mechanistic pathways for the *N*-nitroso piperazine **26** are shown. The activation energies clearly show that *N*-hydroxylation with an activation energy of 10.2 kcal/mol occurs readily followed by *N*-oxidation and α-hydroxylation.[37,38] The AI values obtained from TD50 for *N*-nitroso piperazine **26** is 8780 ng/day which is substantially high compared to that of *N*-nitroso piperidine of 1300 ng/day, whereas CPCA predicts AI of 400 ng/day. The trend in TD50 can be explained well by the consideration of different possible metabolic pathways for nitrosamines. This is yet another example that emphasizes that QM can be used to justify the AI of nitrosamines. Similarly, in the case of **28**, the activation energy for S-oxidation is 13.5 kcal/mol which is substantially lower than the activation energy of C−H activation of 20.2 kcal/mol. It means that *N*-nitroso thiomorpholine preferably undergoes an S-oxidation process compared to that of an α-hydroxylation process which can justify the higher TD50 for **28** compared to **25**. Bruno et al.[39] also identified a similar observation in the case of thiomorpholine where S-oxidation was found to be preferred over C−H oxidation.

Aromatic Nitrosamines. Figure 15 shows the *N*-methyl aryl nitrosamines considered in this study. These molecules have no α−C−H bond on one side of the nitrosamine group and have one CH_3 group on the other side. According to the CPCA, the α-hydrogen score is 2 for compounds **29**−**35**, the overall potency score of 2 belongs to category 2 which corresponds to the recommended levels of 100 ng/day AI. Due to the absence of an α-hydrogen on one side of the nitrosamine group, the α-hydroxylation can potentially occur on the methyl group. The TD50 values are in the range of

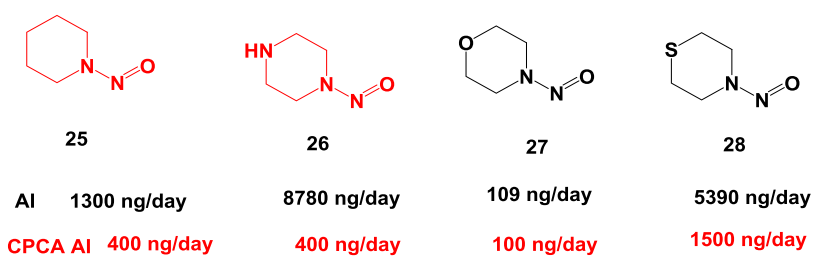

Figure 12. Compounds considered to understand the heteroatom effect on nitrosamine reactivity. AI values estimated from TD50 and CPCA predicted AI limits (in red) are also shown.

https://doi.org/10.1021/acs.chemrestox.4c00087
Chem. Res. Toxicol. 2024, 37, 1011−1022

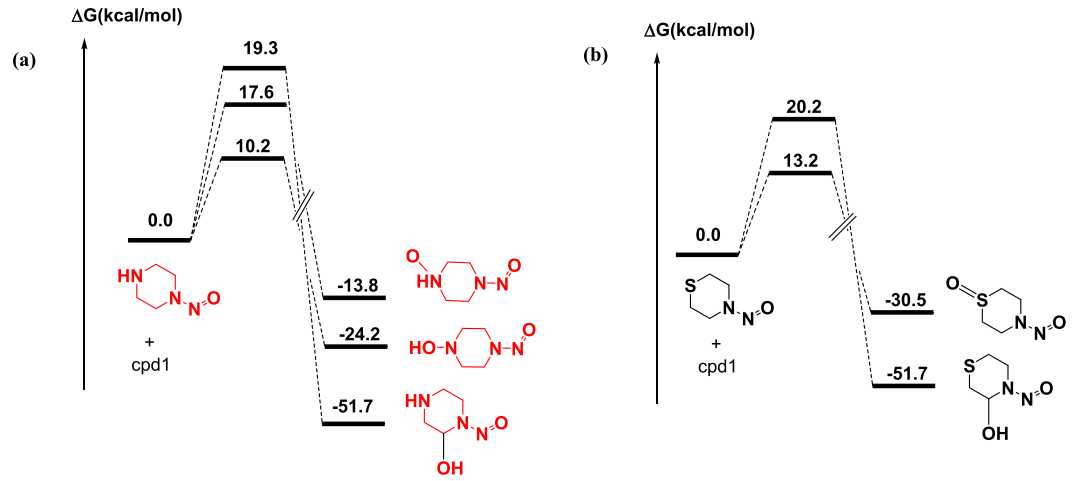

Figure 14. (a) Probable pathways P450 activation mechanism in *N*-nitroso piperazine (b) Probable pathways P450 activation mechanism in *N*-nitroso thiomorpholine.

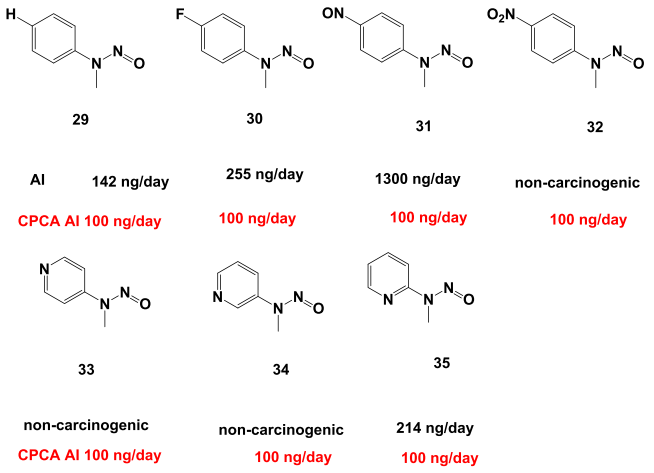

Figure 15. Aromatic nitrosamines considered in the present study.

0.142−1.300 mg/kg/day and two noncarcinogenic molecules **32** and **33**. Thus, the CPCA potency category is significantly conservative for this class of molecules. Nonetheless, we have attempted to understand the reactivity of these aromatics through a carcinogenic metabolic pathway mechanism.

The activation energies ($\Delta G^{\ddagger}_{AB}$) for all of the stepwise reactions involved in the carcinogen metabolic pathway are shown in Table 5. The calculated $\Delta G^{\ddagger}_{AB}$ is in the range of 19.4 (**29**)−21.2 (**30**) kcal/mol for **29**−**34** and considerably high for compound **35** (22.2 kcal/mol), probably because of the steric effect from the N-electron pair. This result clearly indicates that the electron-withdrawing group at the para position influences the steps in the metabolic pathway. Interestingly, the activation energy for the hydrolysis reaction is quite high for all the aromatic reactions except for compound **35** indicating that 2-substituted nitroso pyridine easily undergoes reaction with water. Furthermore, the activation energies for interaction with DNA bases are also observed to be higher for the aromatic molecules but less when compared with the hydrolysis reaction which indicates that aromatic diazonium is more reactive toward DNA bases as compared to water which supports higher potency for these molecular categories when compared with the cyclic saturated nitrosamines.

Table 5. Gibbs Activation Free Energies (in kcal/mol) for All of the Mechanistic Steps Involved in the Aromatic Nitrosamines

nitrosamine	$\Delta G^{\ddagger}_{AB}$	$\Delta G^{\ddagger}_{BC}$	$\Delta G^{\ddagger}_{DE}$	$\Delta G^{\ddagger}_{DG}$
29	19.4	22.4	34.0	28.9
30	21.2	22.3	39.0	35.1
31	20.6	23.1	36.3	31.8
31	20.1	23.8	35.6	30.7
33	20.5	23.3	28.4	22.8
34	20.3	22.9	31.7	27.8
35	22.2	24.1	14.4	11.8

Within the aryl nitrosamine subclass, N-nitroso-*N*-methyl pyridines (NMPYs) (**33**−**35**) present another interesting case study. Even with a subtle difference in structure (i.e., isomers of pyridines), the carcinogenicity changes dramatically from 2-substituted compound **35** being carcinogenic (TD50 of 0.214 mg/kg/day) to 3- and 4-pyridine (**34**, **33** respectively), both being noncarcinogenic. It is well-known that these molecules can undergo a variety of metabolic reactions, one of them being the *N*-oxidation reaction.[28] A study from Eisenbrand[40,41] showed that in the case of substituted *N*-nitroso-*N*-methylpyridines, multiple metabolites are observed. From in vitro studies, they showed that 2-nitroso methylpyridine (2-NMPY) predominantly undergoes α-hydroxylation and 2-hydroxy pyridine is also observed. Our results also indicate that when compared to 3-NMPY (**34**) and 4-NMPY (**33**), the activation energies for the hydrolysis reaction (14.4 kcal/mol for 2-NMPY compared to 28.4 and 31.7 kcal/mol for **34** and **33**, respectively) and DNA base substantially low for 2-NMPY (**35**) as well as for the reaction with DNA base. Breton[42] also observed that 2-pyridyldiazoium cation is more stable than 3-pyridyldiazonium and 4-pyridyl diazonium ion These results clearly differentiate **33**-**35** in terms of the reactivity toward hydrolysis and DNA base. In short, the presence of competing and more accessible alternative CYP450 oxidative pathway results in few of the aromatic nitrosamines being non-carcinogenic, whereas molecules that follow the typical nitrosamine metabolic pathway are carcinogenic, consistent with the mechanism of action and the adverse outcome pathway for nitrosamines.

https://doi.org/10.1021/acs.chemrestox.4c00087
Chem. Res. Toxicol. 2024, 37, 1011−1022

SUMMARY AND CONCLUSIONS

In the present study, we applied QM calculations on dialkyl substituted *N*-nitrosamines, *N*-methyl alkyl nitrosamines, *N*-nitroso pyrrolidines, *N*-nitroso piperidine, *N*-nitroso piperazine, *N*-nitroso morpholine, *N*-nitroso thiomorpholine, *N*-nitroso aromatics to explain the variation in potencies within classes of molecules and to differentiate carcinogenic and noncarcinogenicity metabolic pathways. In most of the nitrosamines studied in this work, the CPCA scores were found to be more conservative than the actual AIs derived from the experimental TD50 values. Specifically, all the *N*-methyl aromatic nitrosamines fall under category 2 which recommends 100 ng/day while the actual TD50 values are higher and nondiscrete. This underscores the need for further refinement of the CPCA where QM modeling can further assist in rationalizing and correcting the AI estimation. While our results broadly support the recent rational classification in the CPCA methodology proposed by EMA and FDA (e.g., the doubly substituted electron-withdrawing groups increase deactivating features thereby decreasing the potency), our QM analysis further showed that electron-withdrawing groups increase the activation energies for all the reactions involved in the carcinogenic metabolism (Figure 5). Furthermore, we have showcased several examples herein where QM modeling provided a meaningful rationale for their reactivity including noncarcinogens, and where CPCA classification falls short.

For the quantitative modeling of TD50 and estimation of AI limits, several studies suggest that local QSAR models using QM parameters can allow for the estimation of AI values.[20,43] In this regard, we have used the evaluation of IR frequency as a surrogate for radical reactivity showing a high correlation to TD50s and used that analysis to support lower potency for several *N*-methyl aromatic NDSRIs (not included in this study). This SAR analysis was supported experimentally by in vivo mutagenicity work (Jolly et al. in progress). These results from QM modeling of mechanistic pathways can be used for weight evidence arguments to support AI estimation of NDSRIs. Additionally, understanding the competitive metabolic pathways for sulfation, glucuronidation, demethylation and denitrosation could potentially help in justifying AI for NDSRIs. Future work will describe other nitrosamine chemistry methods using QM parameters with a focus on competing metabolic pathways.

ASSOCIATED CONTENT

Supporting Information

The Supporting Information is available free of charge at https://pubs.acs.org/doi/10.1021/acs.chemrestox.4c00087.

Cartesian coordinates of all the reactants, intermediates and transition states involved for the molecules 1−35, Gibbs free energy values, and high spin and low spin activation energies for the aromatic molecules (PDF)

Nitrosamine potency information (ZIP)

AUTHOR INFORMATION

Corresponding Authors

Fareed Bhasha Sayyed − *Synthetic Molecule Design and Development, Eli Lilly Services India Pvt Ltd, Bengaluru 560103, India;* orcid.org/0000-0001-8364-4810; Email: sayyed_fareed_bhasha@lilly.com

Robert A. Jolly − *Toxicology, LRL, Eli Lilly and Company, Indianapolis, Indiana 46285, United States;* orcid.org/0000-0001-7106-830X; Email: jolly_robert_a@lilly.com

Authors

Sriman De − *Synthetic Molecule Design and Development, Eli Lilly Services India Pvt Ltd, Bengaluru 560103, India*

Bishnu Thapa − *Discovery Chemistry Research and Technology, LRL, Eli Lilly and Company, Indianapolis, Indiana 46285, United States*

Scott A. Frank − *Synthetic Molecule Design and Development, Eli Lilly and Company, Indianapolis, Indiana 46285, United States;* orcid.org/0000-0001-6680-9695

Paul D. Cornwell − *Toxicology, LRL, Eli Lilly and Company, Indianapolis, Indiana 46285, United States;* orcid.org/0009-0004-9786-774X

Complete contact information is available at: https://pubs.acs.org/10.1021/acs.chemrestox.4c00087

Author Contributions

CRediT: **Sriman De** data curation, formal analysis, methodology, writing-original draft; **Bishnu Thapa** conceptualization, formal analysis, investigation, methodology, writing-original draft; **Fareed Bhasha Sayyed** conceptualization, data curation, formal analysis, investigation, methodology, software, validation, writing-original draft; **Scott A. Frank** investigation, resources, supervision, writing-review & editing; **Paul D Cornwell** writing-review & editing; **Robert A Jolly** conceptualization, investigation, project administration, writing-original draft, writing-review & editing.

Notes

The authors declare no competing financial interest.

ACKNOWLEDGMENTS

The authors thank David Ackley, Douglas Roepke, and Alison Campbell Brewer for reviewing this manuscript. Support from Jon Day for the cover page design.

REFERENCES

(1) Beard, J. C.; Swager, T. M. An Organic Chemist's Guide to N-Nitrosamines: Their Structure, Reactivity, and Role as Contaminants. *J. Org. Chem.* **2021**, *86* (3), 2037−2057.

(2) ICH-M7. *Assessment and Control of DNA Reactive (Mutagenic) Impurities in Pharmaceuticals To Limit Potential Carcinogenic Risk*; ICH, 2017. https://database.ich.org/sites/default/files/M7_R1_Guideline.pdf (accessed on 29th August 2023).

(3) Magee, P. N.; Barnes, J. M. The Production of Malignant Primary Hepatic Tumours in the Rat by Feeding Dimethylnitrosamine. *Br. J. Cancer* **1956**, *10*, 114−122.

(4) Bogovski, P.; Bogovski, S. Animal species in which N-nitroso compounds induce cancer. *Int. J. Cancer* **1981**, *27*, 471−474.

(5) Bartsch, H.; Montesano, R. Relevance of nitrosamines to human cancer. *Carcinogenisis* **1984**, *5*, 1381−1393.

(6) Preussmann, R. *Public health significance of environmental N-nitroso compounds*; IARC Scientific Publication, 1983; Vol. *45*, pp. 3−17.

(7) US FDA. *Announces Voluntary Recall of Several Medicines Containing Valsartan Following Detection of an Impurity*. Available online: https://www.fda.gov/drugs/drug-safety-and-availability/recalls-angiotensin-ii-receptor-blockers-arbs-including-valsartan-losartan-and-irbesartan (accessed on 13th August 2023).

(8) Bharate, S. S. Critical Analysis of Drug Product Recalls due to Nitrosamine Impurities. *J. Med. Chem.* **2021**, *64* (6), 2923−2936.

(9) *Nitrosamine impurities*; European Medicines Agency, **2023**. https://www.ema.europa.eu/en/human-regulatory/post-

authorisation/referral-procedures/nitrosamine-impurities (accessed on 29th November 2023).
(10) *Control of Nitrosamine Impurities in Human Drugs*; FDA, **2023**. https://www.fda.gov/regulatory-information/search-fda-guidance-documents/control-nitrosamine-impurities-human-drugs (accessed on 05 April 2024).
(11) Moser, J.; Ashworth, I. W.; Harris, L.; Hillier, M. C.; Nanda, K. K.; Scrivens, G. N-Nitrosamine Formation in Pharmaceutical Solid Drug Products: Experimental Observations. *J. Pharm. Sci.* **2023**, *112* (5), 1255−1267.
(12) Schlingemann, J.; Burns, M. J.; Ponting, D. J.; Martins Avila, C.; Romero, N. E.; Jaywant, M. A.; Smith, G. F.; Ashworth, I. W.; Simon, S.; Saal, C.; et al. The Landscape of Potential Small and Drug Substance Related Nitrosamines in Pharmaceuticals. *J. Pharm. Sci.* **2023**, *112*, 1287. From NLM Publisher.
(13) Thresher, A.; Foster, R.; Ponting, D. J.; Stalford, S. A.; Tennant, R. E.; Thomas, R. Are all nitrosamines concerning? A review of mutagenicity and carcinogenicity data. *Regul. Toxicol. Pharmacol.* **2020**, *116*, No. 104749.
(14) Bercu, J. P.; Masuda-Herrera, M.; Trejo-Martin, A.; Sura, P.; Jolly, R.; Kenyon, M.; Thomas, R.; Ponting, D. J.; Snodin, D.; Tuschl, G. Acceptable intakes (AIs) for 11 small molecule N-nitrosamines (NAs). *Regul. Toxicol. Pharmacol.* **2023**, *142*, No. 105415. From NLM Publisher.), 142.
(15) Woolley, D. R.; Cross, K. P.; Johnson, G. E. Risk (Re)Assessment of N-Methyl-N-Nitrosophenethylamine for Use in Computing Acceptable Intake Levels of N-Nitrosamine Drug Substance-Related Impurities. In *Toxicologist, a Supplement to Toxicological Science*, **2023**, Abstract #4477.
(16) Oliveiria, A. A.; Martins-Avila, C.; Ponting, D. J.. Collaborative Analysis of Complex Nitrosamines. In *Toxicologist, a Supplement to Toxicological Sciences*, **2023**, Abstract #5063.
(17) Cross, K. P.; Ponting, D. J. Developing structure-activity relationships for N-nitrosamine activity. *Comput. Toxicol.* **2021**, *20*, No. 100186.
(18) Dobo, K. L.; Kenyon, M. O.; Dirat, O.; Engel, M.; Fleetwood, A.; Martin, M.; Mattano, S.; Musso, A.; McWilliams, J. C.; Papanikolaou, A.; et al. Practical and Science-Based Strategy for Establishing Acceptable Intakes for Drug Product N-Nitrosamine Impurities. *Chem. Res. Toxicol.* **2022**, *35* (3), 475−489.
(19) Thomas, R.; Tennant, R. E.; Oliveira, A. A. F.; Ponting, D. J. What Makes a Potent Nitrosamine? Statistical Validation of Expert-Derived Structure−Activity Relationships. *Chem. Res. Toxicol.* **2022**, *35* (11), 1997−2013.
(20) Wenzel, J.; Schmidt, F.; Blumrich, M.; Amberg, A.; Czich, A. Predicting DNA-Reactivity of N-Nitrosamines: A Quantum Chemical Approach. *Chem. Res. Toxicol.* **2022**, *35* (11), 2068−2084.
(21) Ponting, D. J.; Dobo, K. L.; Kenyon, M. O.; Kalgutkar, A. S. Strategies for Assessing Acceptable Intakes for Novel N-Nitrosamines Derived from Active Pharmaceutical Ingredients. *J. Med. Chem.* **2022**, *65*, 15584 DOI: 10.1021/acs.jmedchem.2c01498.
(22) *Recommended Acceptable Intake Limits for Nitrosamine Drug Substance Related Impurities (NDSRIs) Guidance for Industry*. https://www.fda.gov/media/170794/download (accessed on 2nd February 2024).
(23) Personal communication Suman Chakravarti. CEO multicase.
(24) Frisch, M. J.; Trucks, G. W.; Schlegel, H. B.; Scuseria, G. E.; Robb, M. A.; Cheeseman, J. R.; Scalmani, G.; Barone, V.; Petersson, G. A.; Nakatsuji, H.; Li, X.; Caricato, M.; Marenich, A. V.; Bloino, J.; Janesko, B. G.; Gomperts, R.; Mennucci, B.; Hratchian, H. P.; Ortiz, J. V.; Izmaylov, A. F.; Sonnenberg, J. L.; Williams-Young, D.; Ding, F.; Lipparini, F.; Egidi, F.; Goings, J.; Peng, B.; Petrone, A.; Henderson, T.; Ranasinghe, D.; Zakrzewski, V. G.; Gao, J.; Rega, N.; Zheng, G.; Liang, W.; Hada, M.; Ehara, M.; Toyota, K.; Fukuda, R.; Hasegawa, J.; Ishida, M.; Nakajima, T.; Honda, Y.; Kitao, O.; Nakai, H. et al. *Gaussian 16, Revision B.01*; Gaussian, Inc, 2018.
(25) Grimme, S.; Ehrlich, S.; Goerigk, L. Effect of the damping function in dispersion corrected density functional theory. *J. Comput. Chem.* **2011**, *32*, 1456−1465.
(26) Becke, A. D. Density-functional thermochemistry. III. The role of exact exchange. *J. Chem. Phys.* **1993**, *98* (7), 5648−5652.
(27) Lee, C.; Yang, W.; Parr, R.G. Development of the Colle-Salvetti correlation-energy formula into a functional of the electron density. *Phys. Rev. B* **1988**, *37* (2), 785−789.
(28) Ma, G.; Yu, H.; Xu, T.; Wei, X.; Chen, J.; Lin, H.; Schüürmann, G. Computational Insight into the Activation Mechanism of Carcinogenic N'-Nitrosonornicotine (NNN) Catalyzed by Cytochrome P450. *Environ. Sci. Technol.* **2018**, *52* (20), 11838−11847.
(29) Barone, V.; Cossi, M. Quantum Calculation of Molecular Energies and Energy Gradients in Solution by a Conductor Solvent Model. *J. Phys. Chem. A* **1998**, *102* (11), 1995−2001.
(30) Cossi, M.; Rega, N.; Scalmani, G.; Barone, V. Energies, structures, and electronic properties of molecules in solution with the C-PCM solvation model. *J. Comput. Chem.* **2003**, *24* (6), 669−681.
(31) Laidler, K. J.; King, M. C. Development of transition-state theory. *J. Phys. Chem.* **1983**, *87* (15), 2657−2664.
(32) Vaz, A. D. N.; Coon, M. J. On the Mechanism of Action of Cytochrome P450: Evaluation of Hydrogen Abstraction in Oxygen-Dependent Alcohol Oxidation. *Biochemistry* **1994**, *33* (21), 6442−6449.
(33) Puetz, H.; Puchl'ová, E.; Vranková, K.; Hollmann, F. Biocatalytic Oxidation of Alcohols. *Catalysts* **2020**, *10* (952), 952.
(34) Li, Y.; Hecht, S. S. Metabolic Activation and DNA Interactions of Carcinogenic N-Nitrosamines to Which Humans Are Commonly Exposed. *Int. J. Mol. Sci.* **2022**, *23*, 4559.
(35) The activation energies N-oxidation transition state in high-spin and low-spin states are 12.9 and 17.4 kcal/mol respectively. The activation energies N-CH_3 hydroxylation of $N(CH_3)_2$ group transition state in high-spin and low-spin states are 9.2 and 7.4 kcal/mol respectively. The activation energies N-CH_3 hydroxylation of $N(CH_2)$-NNO group transition state in high-spin and low-spin states are 19.0 and 21.1 kcal/mol respectively.
(36) (a) Confer, M. P.; Qu, T.; Rupar, P. A.; Dixon, D. A. Composite Correlated Molecular Orbital Theory Calculations of Ring Strain for Use in Predicting Polymerization Reactions. *ChemPhysChem* **2022**, *23* (9), No. e202200133. (b) Snodin, D. J.; Trejo-Martin, A.; Ponting, D. J.; Smith, G. F.; Czich, A.; Cross, K.; Custer, L.; Elloway, J.; Greene, N.; Kalgutkar, A. S.; et al. Mechanisms of Nitrosamine Mutagenicity and Their Relationship to Rodent Carcinogenic Potency. *Chem. Res. Tox.* **2024**, *37* (2), 181−198.
(37) Ripa, L.; Mee, C.; Sjö, P.; Shamovsky, I. Theoretical Studies of the Mechanism of N-Hydroxylation of Primary Aromatic Amines by Cytochrome P450 1A2: Radicaloid or Anionic? *Chem. Res. Toxicol.* **2014**, *27*, 265−278.
(38) Ji, L.; Schrmann, G. Model and Mechanism: N-Hydroxylation of Primary Aromatic Amines by Cytochrome P450. *Angew. Chem., Int. Ed.* **2013**, *52*, 744−748.
(39) Combourieu, B.; Poupin, P.; Besse, P.; Sancelme, M.; Veschambre, H.; Truffaut, N.; Delort, A.-M. Thiomorpholine and morpholine oxidation by a cytochrome P450 in Mycobacterium Aurum MO1. Evidence of the intermediates by in situ 1H NMR. *Biodegradation* **1998**, *9*, 433−442.
(40) Heydt-Zapf, G.; Haubner, R.; Preussmann, R.; Eisenbrand, G. Metabolism of carcinogenic and non-carcinogenic N-nitroso-N-methylaminopyridines. n. Investigations in vivo. *Carcinogenesis* **1983**, *4* (6), 729−731.
(41) Heydt, G.; Eisenbrand, G.; Preussmann, R. Metabolism of carcinogenic and non-carcinogenic N-nitroso-N-methylaminopyridines. I. Investigations in vitro. *Carcinogenesis* **1982**, *3* (4), 445−448.
(42) Breton, G. W. DFT study of ortho, meta and para−pyridyl cations Pyridynium found? *Comput. Theor. Chem.* **2018**, *1133*, 51−57.
(43) Kostal, J.; Voutchkova-Kostal, A. Quantum-Mechanical Approach to Predicting the Carcinogenic Potency of N-Nitroso Impurities in Pharmaceuticals. *Chem. Res. Toxicol.* **2023**, *36* (2), 291−304.

Regulatory Toxicology and Pharmacology 152 (2024) 105672

Contents lists available at ScienceDirect

Regulatory Toxicology and Pharmacology

journal homepage: www.elsevier.com/locate/yrtph

Estimation of acceptable daily intake values based on modeling and *in vivo* mutagenicity of NDSRIs of fluoxetine, duloxetine and atomoxetine

Robert A. Jolly [a,*], Paul D. Cornwell [a], Jessica Noteboom [a], Fareed Bhasha Sayyed [b], Bishnu Thapa [a], Lorrene A. Buckley [a]

[a] *Eli Lilly and Company, Inc. Indianapolis, IN, 46285, USA*
[b] *Eli Lilly Services India Pvt Ltd, Bengaluru, 560103, India*

ARTICLE INFO

Handling Editor: Martin Van den berg

Keywords:
Nitrosamine
NDSRI
Risk assessment
Quantum mechanical modeling
Transgenic rodent assay
Mutagenicity
Acceptable intake

ABSTRACT

Nitrosamine drug substance related impurities or NDSRIs can be formed if an active pharmaceutical ingredient (API) has an intrinsic secondary amine that can undergo nitrosation. This is a concern as 1) nitrosamines are potentially highly potent carcinogens, 2) secondary amines in API are common, and 3) NDSRIs that might form from such secondary amines will be of unknown carcinogenic potency. Approaches for evaluating NDSRIs include read across, quantum mechanical modeling of reactivity, *in vitro* mutation data, and transgenic *in vivo* mutation data. These approaches were used here to assess NDSRIs that could potentially form from the drugs fluoxetine, duloxetine and atomoxetine. Based on a read across informed by modeling of physicochemical properties and mechanistic activation from quantum mechanical modeling, NDSRIs of fluoxetine, duloxetine, and atomoxetine were 10-100-fold less potent compared with highly potent nitrosamines such as NDMA or NDEA. While the NDSRIs were all confirmed to be mutagenic *in vitro* (Ames assay) and *in vivo* (TGR) studies, the latter data indicated that the potency of the mutation response was ≥4400 ng/day for all compounds-an order of magnitude higher than published regulatory limits for these NDSRIs. The approaches described herein can be used qualitatively to better categorize NDSRIs with respect to potency and inform whether they are in the ICH M7 (R2) designated Cohort of Concern.

1. Introduction

Nitrosamine drug substance related impurities or NDSRIs, are a significant issue for pharmaceutical manufacturers, as they can form whenever an active pharmaceutical ingredient (API) or intermediate in its synthetic route has an intrinsic secondary amine that can undergo nitrosation (Moser et al., 2023; Schlingemann et al., 2022). Control of NDSRIs is challenging because these impurities can form over the lifetime of a medicine (Nudelman et al., 2023) and are currently regulated at very low limits. Recently the FDA and EMA have promoted the carcinogenic potency categorization approach (CPCA; USFDA, 2023; EMA, 2023) for assessment of NDSRIs. The CPCA is an algorithm methodology promoted by health authorities for use in AI (Acceptable Intake) determination using structural features of NDSRIs (Kruhlak et al., 2024). While many NDSRIs are not potent carcinogens like low molecular weight (LMW) nitrosamines (Thresher et al., 2020), the CPCA nevertheless classifies many NDSRIs as being equivalent to or more potent than NDEA or NDMA (USFDA, 2023; EMA, 2023). This level of conservatism in setting acceptable limits overestimates the safety concern and has led to unnecessary market withdrawals, as manufacturers struggle to meet stringent and possibly analytically unfeasible limits for NDSRIs in their products (Nudelman et al., 2023; Burns et al., 2023).

Read across approaches were initially used to estimate AIs for NDSRIs. Embedded in such approaches are computational methods for comparing both structure similarity and physicochemical properties. However, the differences in MW and other properties between NDSRIs and LMW nitrosamines are significant (Oliveiria et al., 2023), and simple 2-dimensional similarity or considering molecular weight alone may overestimate the risk (Fine et al., 2023). Nonetheless, this methodology was used holistically to find the best surrogate nitrosamine to a given NDSRI to approximate an AI. Understanding of the mecshanism and adverse outcome pathway for nitrosamines further allowed used of quantum mechanical (QM) assessments of the steps of nitrosamine

* Corresponding author.
E-mail address: Jollyra@lilly.com (R.A. Jolly).

https://doi.org/10.1016/j.yrtph.2024.105672
Received 1 May 2024; Received in revised form 19 June 2024; Accepted 28 June 2024
Available online 4 July 2024

activation, e.g. hydroxylation and reactive intermediate formation and reactivity. Such computational approaches including QM calculations are shown in this manuscript for three NDSRIs. Understandably, gaining regulatory acceptance of such novel approaches in read across remains a challenge and uptake has been slow, although the recent structure activity relationship (SAR) work (Cross and Ponting, 2021) has been instrumental in forming the basis of and improving upon the CPCA.

NDSRIs formed during the synthesis of drug substance can be more readily qualified through carcinogenicity assessment of the API which contains the NDSRI impurity than NDSRIs that form subsequently in drug product due to the presence of nitrosating agents in excipients or from other sources. Many NDSRIs are qualified *in vitro* using the Ames assay described in OECD Guideline 471 (Heflich et al., 2020; OECD guidelines 471, 2020). However, that Ames assay has been called into question by Health Authorities (HAs) as not sensitive enough for nitrosamines, despite data indicating it is as or more predictive for assessing nitrosamine mutagenicity than for other mutagenic compounds (Trejo-Martin et al., 2022). Accommodations to the assay to address perceived deficiencies, such as including increased amount of S9, the use of hamster S9, and a longer preincubation for enhanced bioactivation, have been implemented (FDA, 2023; EMA, 2023). A negative result from this updated version of the Ames test, termed the Enhanced Ames Test (EAT) in some regulatory guidelines, has allowed for increased limits for NDSRIs (FDA, 2023; EMA, 2023) but only to the threshold of toxicological concern and not to the level of an ordinary impurity per ICH Q3A/B.

An inability to sufficiently de-risk NDSRIs with the Ames assay has led pharmaceutical companies to test NDSRIs in transgenic rodent models, such as the Big Blue® or Mutamouse® to assess the potential for mutation (Schmezer et al., 1998; Jacobson-Kram et al., 2004). These *in vivo* mutagenicity assays, which are validated and conducted according to regulatory guidelines (OECD 488 2022) and Good Laboratory Practices (GLPs), are considered adequate to qualify the mutagenic potential of impurities (ICH M7 (R2) 2023) although, despite the high demand, only a limited number of laboratories are currently capable of conducting such studies. Although studies such as the Ames assay and transgenic rodent studies have been employed for qualitative hazard assessment, their use for quantitative risk assessment use was discouraged in the ICH M7 (R2) Guidance Q&A (ICH, 2023) and has not been commonly employed to date. Historically, the literature indicates that *in vitro* potency in the Ames assay is not strongly correlated with carcinogenic potency (Purchase, 1985; McCann et al., 1988), the opposite appears to be true for *in vivo* transgenic mutation data (Aoki 2017). One path forward for evaluation of NDSRIs impurities is to use a relative potency approach based on AIs generated using *in vivo* rodent mutagenicity studies. At the least, such an approach could be used qualitatively to better categorize NDSRIs with respect to potency, e.g., to inform whether they are in the ICH M7 (R2)-designated Cohort of Concern (ICH, 2023). The data can additionally be employed in a more quantitative manner, e.g., to derive more meaningful AI limits. The current paper describes an evaluation of NDSRIs that can potentially form in Prozac® (fluoxetine), Cymbalta® (duloxetine), and Strattera® (atomoxetine) - three highly structurally similar examples of the oxetine drug family and which have been commercially available for decades. These drugs are selective reuptake inhibitors of the neurotransmitters: serotonin (SSRI, fluoxetine), serotonin and norepinephrine (SSRI/SNRI, duloxetine), and norephinephrine (SNRI, atomoxetine) and are prescribed for the treatment several neurological disorders (FDA 2022, 2023a, 2023b). Herein, we describe the derivation of AIs for the nitrosated forms of each drug using computational assessments, read across methodology, and *in vivo* mutation data for these potential impurities. Furthermore, these analyses demonstrate that *in vivo* mutation data can be used to derive a conservative and quantitative AI for NDSRI molecules.

2. Materials and methods

The structures and Lilly serial numbers (LSNs) for fluoxetine, duloxetine, and atomoxetine as well as the NDSRIs for each API are shown in Fig. 1. LSNs of the NDSRIs are LSN3868255 for N-nitroso fluoxetine (NFLX), LSN3868254 for N-nitroso duloxetine (NDLX) and LSN3868306 for N-nitroso atomoxetine (NATX) respectively and all LSNs were synthesized at Wuxi labs (China) with a purity greater than 99%.

2.1. Computational assessments based on structure and physicochemical properties

Computational assessments, including structure and substructure similarity and physicochemical property calculations on the NDSRIs, were conducted using both Leadscope Model v3.0.2–4 (Columbus, OH) and QSARflex software v1.6 (Mayfield, OH) programs.

2.2. Quantum mechanical modeling

For the quantum mechanical (QM) modeling, TD_{50}[1] values from compounds with structural similarity to the NDSRIs were collected from the Lhasa carcinogenicity database (Lhasa Carcinogenicity Database (lhasalimited.org). In particular, the compounds bearing similar structural and electronic features of these NDSRIs, such as those compounds with or without an oxygen substitution at the β and γ carbon atoms as well as compounds with an electron withdrawing group (EWG; e.g. CF_3), were included in this analysis. All computational calculations were performed using the Gaussian 16 suite of programs (Frisch, 2016). Geometrical structures of molecules were optimized using density functional theory i.e., at the M062X/6-31+G (d,p) level of theory (Zhao and Truhlar, 2008). Previous reports indicate that M062X function

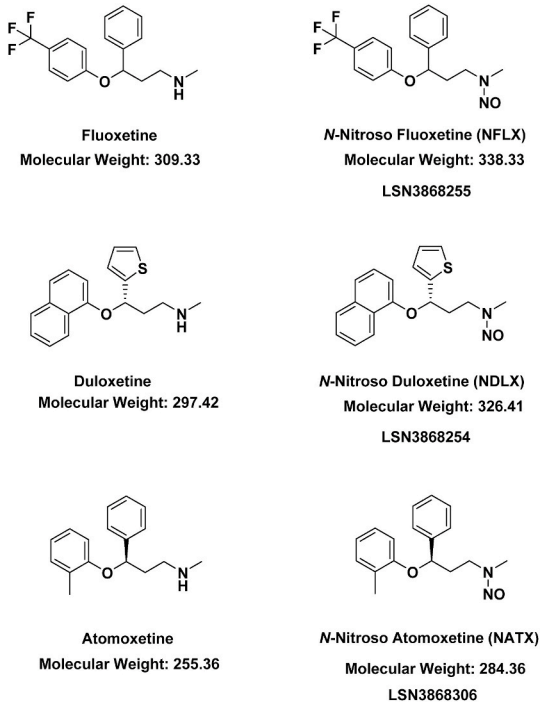

Fig. 1. Structures of APIs and NDSRIs.

[1] The TD50 is defined as the dose required to halve the probability of a subject (animal) remaining without tumors throughout a lifetime of exposure.

performs well for thermochemistry and reactivity of organic molecules (Zhao and Truhlar, 2008; López-López and Ayala, 2016; Park and Kang, 2019; Walker et al., 2013; Mardirossian and Head-Gordon, 2016). Vibrational frequency calculations were performed on the optimized structures at M062X/6-31+G (d,p) level of theory to verify the optimized geometries are actual minima on the potential energy surface, and therefore no negative frequencies are observed. Since the stretching vibrational frequencies are well correlated with bond dissociation energies, which in turn are indicative of relative stability of the bond (Finkelshtein, 1999), the C—N═N infrared stretching frequency of diazo compounds was considered the QM descriptor and was correlated with TD_{50} for all molecules.

2.3. Bacterial reverse mutation (Ames) assay

NFLX, NATX, and NDLX were tested in the bacterial reverse mutation (Ames) assay (BioReliance, Rockville, MD) or LabCorp (Harrogate, UK). All testing was done per OECD 471 protocol (OECD 471 2022) and under GLP compliance using five tester strains. Given that nitrosamines are known to require metabolic activation, a twenty or 30-min pre-incubation was incorporated into the study design using both rat and hamster S9 metabolic activation systems (10%) to ensure metabolic competency of the assay. Acetonitrile was used as a vehicle.

2.4. Transgenic rat mutagenicity (TGR) studies

The TGR study used transgenic F344 rats that contain multiple copies of chromosomally integrated *cII* gene of the lambda bacteriophage shuttle vector. The transgenes contain reporter genes for the detection of various types of mutations induced *in vivo* by test chemicals (OECD 488 2022). All phases of the TGR studies were compliant with regulatory guidelines (OECD 488 2022) and GLPs. A concurrent positive control group treated with N-ethyl-N-nitrosourea was also included to verify the validity of the assay. The dosing and live phases of the studies were completed at Charles River Laboratory (Ashland, OH). NDSRIs were administered to male and female (wild type) F344 rats in seven-day range finding studies to determine maximally tolerated doses for the subsequent 28-day mutagenicity studies. In the range finding studies, rats were dosed at 30, 100, 300 and 1000 mg/kg, p.o. with the highest dose being a limit dose according to the OECD 488 guideline. The liver and duodenum are standard tissues assessed under the OECD 488 guideline which emphasizes the need to consider route of administration and drug disposition in tissue selection. The liver is considered a relevant target for nitrosamine carcinogenicity as it is the primary site for metabolic activation for NDSRIs, while the duodenum is relevant for being a site of first contact following oral administration.

Based on the results of the range finding studies, male transgenic F344 rats were treated with each NDSRI for 28 days at doses of 0 (vehicle), 0.1. 0.537, 5, 30 and 100 mg/kg p.o followed by a 3-day washout period (OECD 488 2022). At termination, samples of liver and duodenum were flash frozen, stored on dry ice and shipped to Gentronix (Cheshire, UK) for DNA isolation and mutation frequency analysis. The liver is the primary site of metabolism/bioactivation and the tumor target tissue for nitrosamines, while duodenum is one of the initially exposed tissues following the oral route of administration and has a rapidly dividing cell population. Additionally, the liver is a primary concern for the carcinogenic response of many LMW ntirosamines. DNA was extracted from frozen liver and duodenum samples based on methods described for Agilent product RecoverEase™ (Agilent Technologies, 2018). Subsequent *cII* mutation frequency analysis was based on the Agilent instruction manual 'λ Select-cII Mutation Detection System for Big Blue Rodents' (Agilent Technologies, 2015b), the Agilent instruction manual 'Transpack Packaging Extract for Lambda Transgenic Shuttle Vector Recovery' (Agilent Technoliges, 2015a), and the OECD 488 transgenic study protocol (OECD 488 2022).

Analysis of mutation data was performed using GraphPad Prism v9.3.1. Statistical analyses were conducted on the $\log_{10}$-transformed mutant frequencies for each tissue type separately. A test article was considered positive for inducing *cII* gene mutations if.

- it induced a statistically significant increase in the frequency of *cII* gene mutants at any dose level compared with the concurrent negative control,
- when evaluated for trend, the results were dose-related, and
- the mutant frequency in any treatment group was outside the upper 95% (>2 standard deviations across studies) control limit of the historical negative control mutant frequency distribution for the tissue type in this assay

For positive test articles, a no-observed effect level (NOEL) for *in vivo* mutagenicity was determined. In addition, a benchmark dose (BMD) analysis of the mutation data was done using EPA software version 2.73. The response rate was set at 0.5 standard deviations per EPA and EFSA recommendations for endpoints of concern (Hardy et al., 2017; EPA, 2012). In this way, a Benchmark Dose-Low (Lower 95% confidence limit; BMDL) was determined for each NDSRI. Tabular results of the mutation and BMD data can be found in the supplementary material.

3. Results

3.1. Computational assessments based on structure and physicochemical properties

The NDSRIs were compared to other nitrosamine compounds in the Lhasa database based on structure, substructure similarity, and selected physiochemical properties. The results of those comparisons are shown in **Table 1**. Using both Leadscope and QSARFlex, the closest nitrosamine analogs in the Lhasa database were NNAL and NNK based purely on 2D structure. The similarity scores based on local alert environment in **Table 1** (e.g. the alkyl nitrosamine) were higher than whole structure similarity. NNAL and NNK remained the closest compounds to the NDSRIs for substructure similarity though by not as wide a margin as for whole structure similarity. Importantly, and as shown in **Table 1**, the predicted LogP and predicted water solubility values were dramatically different for NNAL and NNK when compared to the NDSRIs being assessed. For an impurity of a drug given orally, solubility can be considered especially important in terms of impacting potential exposure. Additionally, other physiochemical properties including molecular weight, hydrogen bond donors, hydrogen bond acceptors, parent atoms, molecular weight, polar surface area, and rotatable bonds were assessed and also suggested that NNK and NNAL were not the best surrogates (data not shown). Based on physicochemical properties and other similarity metrics, other nitrosamine compounds including alkylamines such as N-nitroso N-methyl dodecylamine could reasonably be viewed as better surrogates for potency to the NDSRIs. N-nitroso N-methyl dodecylamine has the lowest TD_{50} (0.537 mg/kg) among the nitroso alkylamines listed, and that value would result in an AI value of 537 ng per day for these NDSRIs as described in ICH M7 (R2) (ICH, 2023).

Another more general approach to AI estimation was done by averaging the TD_{50} values of the most similar nitrosamines (n = 9) (Table 1). The tenth compound, N-nitroso ephedrine, was removed, as its TD_{50} was much higher than the other nitrosamines, and it was considered an outlier. This exclusion of the TD_{50} of N-nitroso ephedrine significantly decreased the average TD_{50} and thus provided a more conservative estimate of the average TD_{50} value. This assessment gave an average TD_{50} of approximately 1 mg/kg, ten-fold higher than the value for NNK. While this approach cannot be considered analytical, it does give an approximate AI for the nearest similar structures and supports a higher overall AI. This analysis also highlights the challenges for estimating AIs for NDSRI.

Table 1
Tanimoto structural similarity for NDSRIs and selected physicochemical properties of top ten nearest neighbors nitrosamines from QSARFlex.

	Name	CAS Number	Alert Env. Similarity	Whole Structure Similarity	Mol. Wt.	CPDB TD50 (mg/kg/day)	PredictedLogP	Predicted Water Solubility (gm/L)
NFLX LSN3868255	N-Nitroso fluoxetine	150494-06-7	1	1	338.3	–	4.15	0.003
	4-(methyl nitrosoamine)-1-(3-pyridy)-1-butanol (NNAL)	76014-81-8	0.65	0.468	209.2	0.103	0.27	443.23
	4-(methyl nitrosoamine)-1-(3-pyridy)-1-butanone (NNK)	64091-91-4	0.65	0.333	207.2	0.1	0.4	42.031
	Nitrosomethyl-(2-phenylethyl)amine (NMPEA)	13256-11-06	0.608	0.439	164.2	0.01	1.69	4.173
	N-Nitroso-N-methyl-n-dodecylamine	55090-44-3	0.6	0.288	228.4	0.537	5.1	0.004
	N-Nitrosomethylundecylamine	68107-26-6	0.6	0.288	214.4	2.37	4.84	0.007
	N-Nitrosomethyl-(3-hydroxypropyl) amine	70415-59-7	0.6	0.288	118.1	1.66	−0.43	439.982
	N-Nitrosomethyltetradecylamine	75881-20-8	0.6	0.288	256.4	1.65	5.63	0.001
	N-Nitrosomethyldecylamine	75881-22-0	0.6	0.288	200.3	1.26	4.01	0.044
	4-(methylnitrosoamino)-butyric acid	61445-55-4	0.6	0.27	146.1	0.982	−0.45	242.674
					Mean	0.96		
NDLX LSN3868254	N-Nitroso duloxetine	2680527-91-5	1	1	326.4	–	4.31	0.002
	4-(methyl nitrosoamine)-1-(3-pyridy)-1-butanol (NNAL)	76014-81-8	0.661	0.382	209.2	0.103	0.27	443.23
	4-(methyl nitrosoamine)-1-(3-pyridy)-1-butanone (NNK)	64091-91-4	0.661	0.294	207.2	0.1	0.4	42.031
	N-Nitroso-N-methyl-n-dodecylamine	55090-44-3	0.6	0.209	228.4	0.537	5.1	0.004
	N-Nitrosomethylundecylamine	68107-26-6	0.6	0.209	214.4	2.37	4.84	0.007
	N-Nitrosomethyl-(3-hydroxypropyl) amine	70415-59-7	0.6	0.209	118.1	1.66	−0.43	439.982
	N-Nitrosomethyltetradecylamine	75881-20-8	0.6	0.209	256.4	1.65	5.63	0.001
	N-Nitrosomethyldecylamine	75881-22-0	0.6	0.209	200.3	1.26	4.01	0.044
	4-(methylnitrosoamino)-butyric acid	61445-55-4	0.6	0.202	146.1	0.982	−0.45	242.674
	Nitrosomethyl-(2-phenylethyl)amine (NMPEA)	13256-11-06	0.527	0.29	164.2	0.01	1.69	4.173
					Mean	0.96		
NATX LSN3868306	N-Nitroso atomoxetine	3028194-77-3	1	1	284.4	–	3.76	0.021
	4-(methyl nitrosoamine)-1-(3-pyridy)-1-butanol (NNAL)	76014-81-8	0.65	0.451	209.2	0.103	0.27	443.23
	4-(methyl nitrosoamine)-1-(3-pyridy)-1-butanone (NNK)	64091-91-4	0.65	0.322	207.2	0.1	0.4	42.031
	Nitrosomethyl-(2-phenylethyl)amine (NMPEA)	13256-11-06	0.608	0.42	164.2	0.01	1.69	4.173
	N-Nitroso-N-methyl-n-dodecylamine	55090-44-3	0.6	0.275	228.4	0.537	5.1	0.004
	N-Nitrosomethylundecylamine	68107-26-6	0.6	0.275	214.4	2.37	4.84	0.007
	N-Nitrosomethyl-(3-hydroxypropyl) amine	70415-59-7	0.6	0.275	118.1	1.66	−0.43	439.982
	N-Nitrosomethyltetradecylamine	75881-20-8	0.6	0.275	256.4	1.65	5.63	0.001
	N-Nitrosomethyldecylamine	75881-22-0	0.6	0.275	200.3	1.26	4.01	0.044
	4-(methylnitrosoamino)-butyric acid	61445-55-4	0.6	0.26	146.1	0.982	−0.45	242.674
					Mean	1.07		

3.2. Quantum mechanical (QM) modeling

Quantum mechanical modeling was also used to predict TD_{50} values for NFLX, NATX and NDLX. The QM modeling was based on the current understanding of the P450-bioactivation mechanism and subsequent reaction pathways, assuming alpha hydroxylation triggers the metabolic pathway that leads to the diazonium formation which in turn releases N_2 and the resulting alkyl cation reacts with DNA. Fig. 2 depicts a mechanistic pathway with formation of a diazonium intermediate in Step IV and a DNA adduct in Step V, which leads to carcinogenic activity. The disassociation of the C–N bond in the diazonium intermediate in Step IV is crucial for the DNA adduct in Step V as this step directly quantifies the reaction with DNA bases. One measure of the strength of the C–N bond is its bond dissociation energy. Bond dissociation energies are well

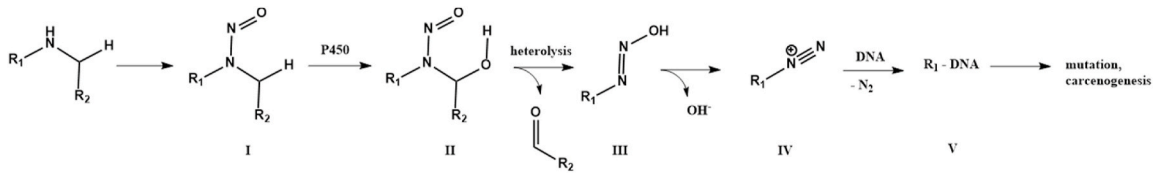

Fig. 2. Cytochrome P450 catalyzed mechanism of potential DNA damage by dialkyl nitrosamines.

correlated to stretch vibrational frequencies measured by infrared (IR) spectroscopy. Therefore, we selected C–N stretching frequencies as a QM descriptor and attempted to find correlation with TD_{50}. Based on both the structural similarity of the chemicals and known metabolism of the APIs, it was considered that alpha hydroxylation would be similar across the NDSRIs and therefore not as impactful to the overall metabolic activation.

The C–N bond stretch vibrational frequencies of the diazonium intermediates formed from the nitrosamines shown in Fig. 3 are evaluated. Compounds with or without an oxygen substitution at the β and γ carbon atoms, an EWG group at these positions, or an aromatic group were included in this analysis (Fig. 3)

The calculated frequencies of the various diazonium intermediate C–N bonds showed a strong correlation with their respective TD_{50} values: correlation coefficient = 0.89 as shown in Fig. 4. This quantum mechanical modeling predicted a TD_{50} of 1.14, 1.15 and 1.19 mg/kg for NFLX, NATX and NDLX respectively as shown in Table 2.

3.3. *Bacterial reverse mutation (Ames) assay*

The results of the *in vitro* mutation Ames assay for the NDSRIs are shown in Table 3. All three NDSRIs were positive in strains associated with point mutations (TA100 or TA1535) in both induced rat and hamster S9 conditions. Consistent with other nitrosamines (Bringezu and Simon, 2022), it was evident that metabolism was largely required for activation and that the strains that were positive were those sensitive to point mutation. Assay sensitivity was enhanced with the hamster (vs rat) S9, but rat S9 also yielded a positive response for all NDSRIs. The positive Ames data for the NDSRI compounds indicated that they have the potential to be carcinogenic. These results confirmed the need for a sensitive analytical method for detection of these NDSRIs in the drug product.

3.3.1. *Transgenic rat mutagenicity study*

In the 7-day range finding studies, clinical observations of toxicity and decreases in body weight, body weight gain, and food consumption demonstrated that 100 mg/kg dose was the maximal tolerated dose

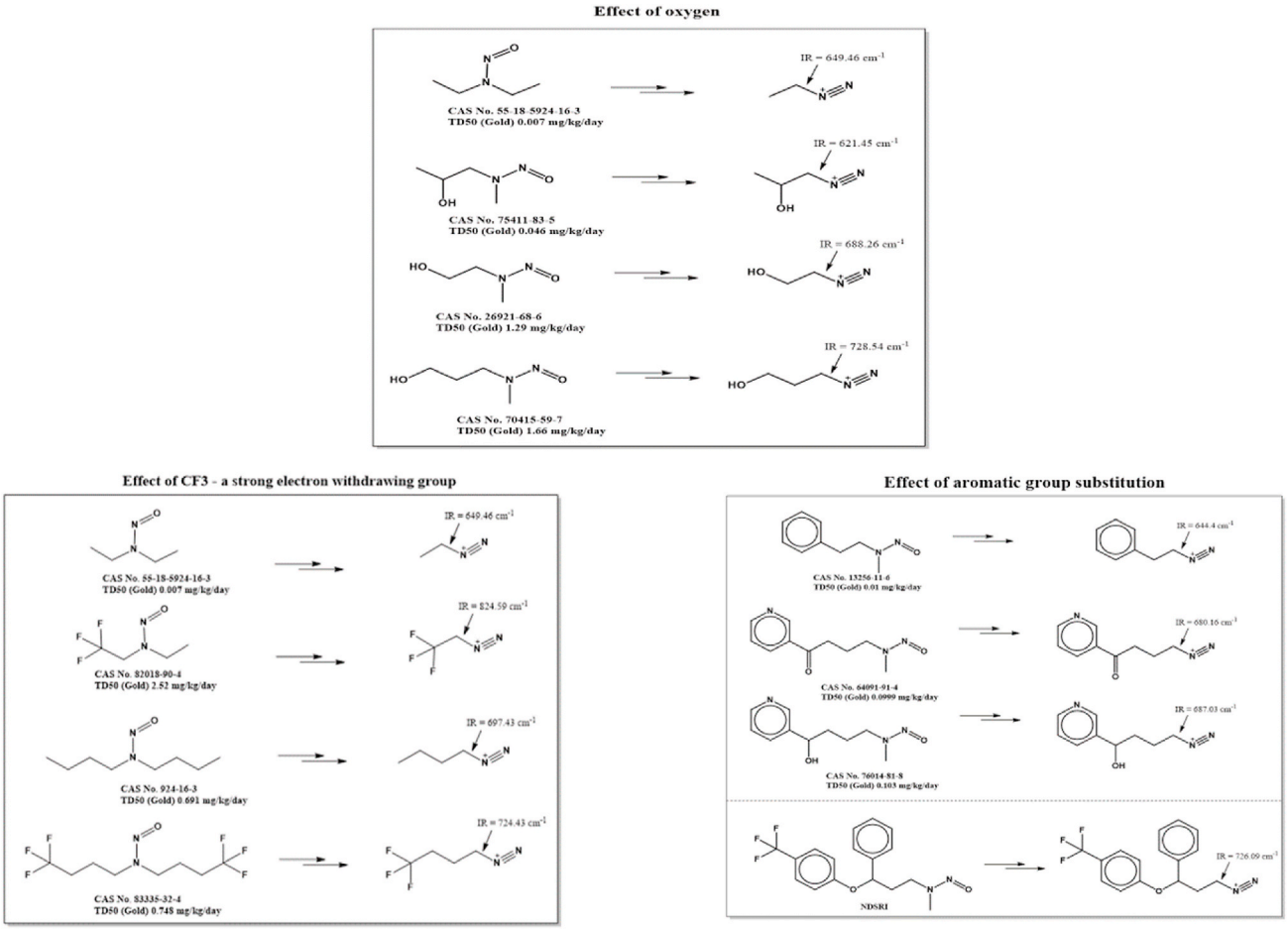

Fig. 3. Parent compounds, putative diazonium intermediates, and infrared (IR) stretching frequencies of the C–N bond of the diazonium intermediates for close analogs of fluoxetine NDSRI based on structural and electronic similarity.

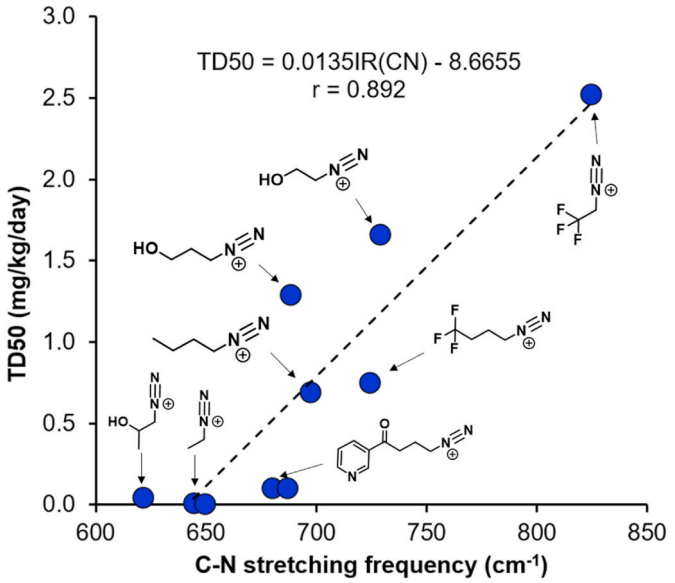

Fig. 4. Correlation of infrared (IR) stretching frequencies of the C–N bond of the diazonium intermediates to TD_{50} for close analogs of fluoxetine NDSRI based on structural and electronic similarity.

Table 2
Infrared Frequencies of the C–N Bond of the Diazonium Intermediates and TD50 Values for Close Analogs of NDSRIs based on Structural and Electronic Similarity.

COMPOUND ID	CAS No.	IR frequency of the diazonium intermediate C–N bond (cm-1)	TD50 (mg/kg/day)
NMIP–OH–A	75411-83-5	621.5	0.046
NMPEA	13256-11-6	644.4	0.010
NDEA	55-18-5	649.5	0.026
NNK	76014-81-	680.2	0.100
NNAL	64091-91-4	687.	0.103
NME–OH–A	70415-59-7	688.3	1.290
NDBA	924-16-3	697.4	0.691
NDBA-CF3	83335-32-4	724.4	0.748
N-nitroso fluoxetine (NFLX)	150494-06-7	726.1	1.140[a]
N-nitroso atomoxetine (NATX)	3028194-77-3	726.6	1.152[a]
N-nitroso duloxetine (NDLX)	2680527-91-5	729.4	1.190[a]
NMP–OH–A	26921-68-6	729.0	1.660
NEE-CF3A	82018-90-4	824.6	2.520

[a] Modeled TD50 values.

(MTD) for all three NDSRIs (data not shown/supplemental). Per OECD 488 testing guideline (OECD 488 2022), 100 mg/kg was chosen as the maximum dose for the definitive 28-day mutagenicity studies. The 7-day studies confirmed exposure of the NDSRIs in both sexes and demonstrated that males were suitable to test in the definitive mutagenicity study (data not shown/supplemental).

Fig. 5 a-c shows the body weight data from the 28-day study for NFLX, NDLX and NATX respectively. The data show a consistent

Table 3
Summarized ames results for N-nitroso fluoxetine (NFLX: LSN3868255) N-nitroso duloxetine (NDLX: LSN3868254) and N-nitroso atomoxetine (NATX: LSN3868306).

	Metabolic Activation:	**None**	**Induced Rat S9 (10%)**	**Induced Hamster S9 (10%)**
NFLX LSN3868255	**Strains and Result:**	TA98: Negative TA100: Negative TA1535: Negative TA1537: Negative WP2uvrA: Negative	TA98: Negative TA100: Positive TA1535: Positive TA1537: Negative WP2uvrA: Positive	TA100: Positive TA1535: Positive
	Metabolic Activation:	**None**	**Induced Rat S9 (10%)**	**Induced Hamster S9 (10%)**
NDLX LSN3868254	**Strains and Result:**	TA98: Negative TA100: Negative TA1535: Negative TA1537: Negative WP2uvrA: Negative	TA98: Negative TA100: Negative TA1535: Positive TA1537: Negative WP2uvrA: Negative	TA100: Positive TA1535: Positive
	Metabolic Activation:	**None**	**Induced Rat S9 (10%)**	**Induced Hamster S9 (10%)**
NATX LSN3868306	**Strains and Result:**	TA98: Negative TA100: Negative TA1535: Negative TA1537: Negative WP2uvrA: Negative	TA98: Negative TA100: Negative TA1535: Positive TA1537: Negative WP2uvrA: Negative	TA100: Positive TA1535: Positive

decrease in body weight at the 100 mg/kg dose for all three NDSRIs, which is consistent with the recommendations of OECD Guideline 488, paragraph 37and confirms the adequacy of the high dose selection.

Mutation data for liver and duodenum are shown in Fig. 6a and b, respectively. Tabular results of the mutation data can be found in the supplementary material. In liver, there was a clear and statistically significant increase in mutation frequency at 30 mg/kg for all three NDSRIs. Thus, this dose represents the lowest observed effect level (LOEL). The 5-mg/kg dose was the NOEL in liver for all three NDSRIs. In all cases, there was a clear threshold in the dose-mutation frequency response. In liver, NFLX had the strongest mutation response followed by NDLX and NATX. This response was observed at the MTD of 100 mg/kg for all three compounds. The general toxicology data (body weight, body weight gain, food consumption) for all compounds was remarkably similar (data not shown).

In the duodenum, there was a statistically significant increase in mutation frequency at the 30- (NATX) and 100-mg/kg doses (NDLX and NATX) but not for NFLX. While mutation frequency of NATX was statistically elevated in duodenum at 5 mg/kg, the mutation frequency for individual animals fell within 95% control limits of historical vehicle control data and the increase in frequency was less than 2-fold that of the concurrent vehicle control. Moreover, the vehicle control duodenum mutant frequency data were notably lower than the laboratory historical vehicle control mean mutant frequency data. For these reasons, the mutation response at 5 mg/kg was considered of questionable biological relevance.

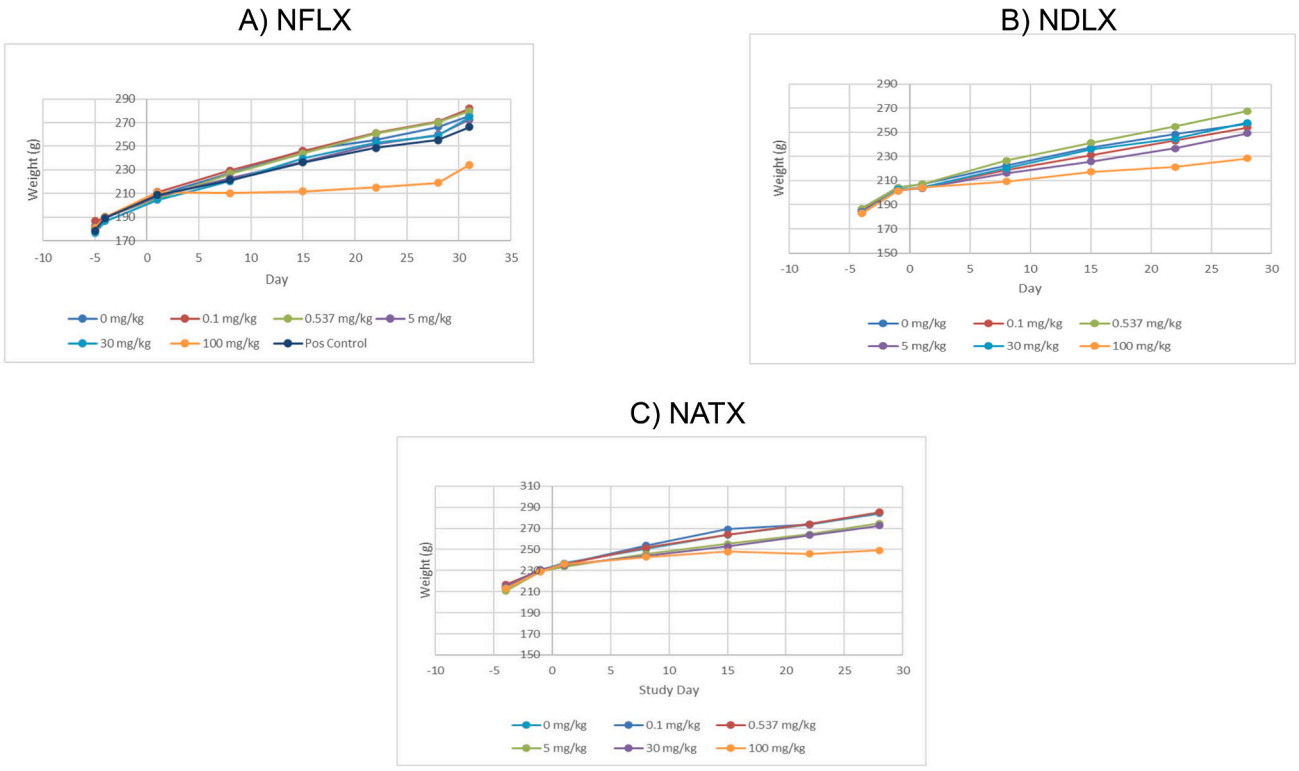

Fig. 5. a-c. Body Weight Data from the 28-Day Studies.

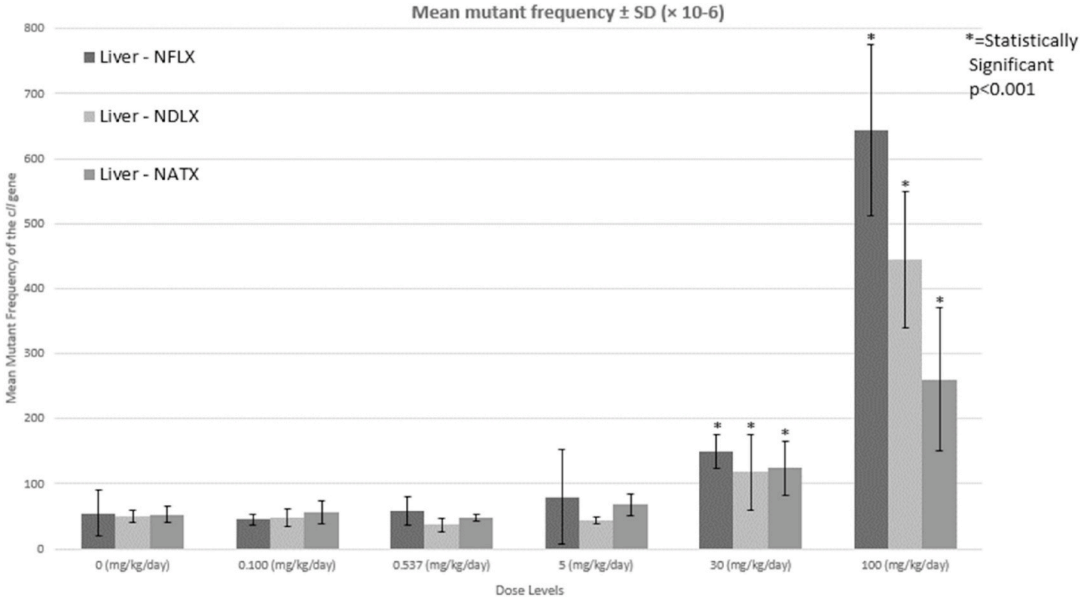

Fig. 6a. Mutation data - liver.

3.4. Benchmark dose analysis

The BMD analysis for the mutation data was performed for liver, as that tissue was the most sensitive in terms of both dose and response. The BMDL values for liver were 6.3, 6.8 and 4.4 mg/kg for NFLX, NDLX and NATX respectively. These BMDL values were generally consistent with the NOEL of 5 mg/kg for all three NDSRIs.

Table 4 shows a summary of NOEL, BMDL, BMD and BMDU values for NDEA and NDMA from the literature as well as the data from the current studies on NDSRIs. The data show that NOEL and BMDL values for the three NDSRIs range from 10 to 100-fold higher than those for NDMA or NDEA, indicating significantly lower potency of the NDSRIs

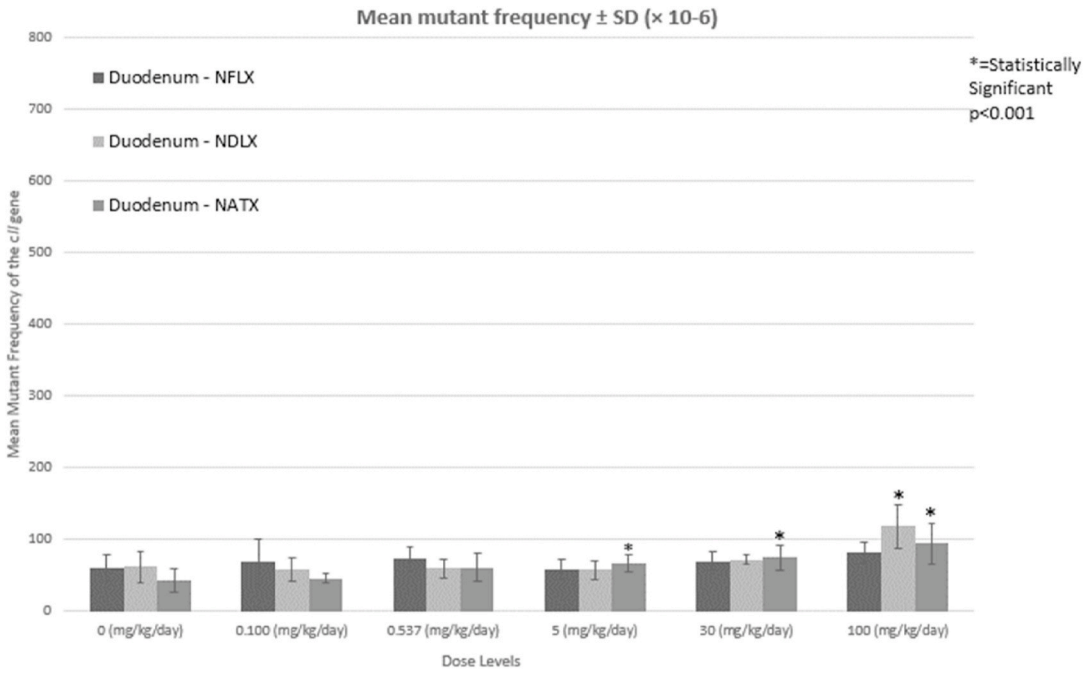

Fig. 6b. Mutation data – duodenum.

Table 4
NOEL, BMDL, BMD and BMDLValues for NDEA, NDMA and NDSRIs.

Agent	Liver NOEL (mg/kg)	Liver BMDL (mg/kg)	Liver BMD (mg/kg)	Liver BMDU (mg/kg)	TD50* (mg/kg)	Reference
NDEA	0.09	0.022	NR	NR	0.0265	Akai (2015)
NDEA	0.1	0.1	NR	1	0.0265	Bercu et al. (2023a, b)
NDMA	0.36	0.21	0.32	0.46	0.096	Gollupadi (1998); Johnson et al. (2021); Lynch et al. (2024)
NFLX	5	6.3	11.4	24.9	ND	Current paper
NDLX	5	6.8	13	24.7	ND	Current paper
NATX	5	4.4	8.7	29.3	ND	Current paper

ND = No data available; NR = Not reported.
*TD50 values based on Lhasa Carcinogenicity database.

compared to those potent nitrosamines.

Published regulatory AIs, CPCA AIs, and AIs for these nitrosamines based on alternate read across and modeling approaches are shown in Table 5.

The CPCA approach, which is based on the nitrosamine structure only, would give the lowest-bin AI value for all 3 NDSRIs: 18 or 26.5 ng/day. The regulatory values published for NFLX, NDLX and NATX are based on a simple 2D structure read across methodology to NNK. As shown in the table, newer, non-traditional methods for AI assessment, such as read across methods using physicochemical properties/QM modeling/or an AI derived from *in vivo* mutation data all indicate lower potencies and substantially higher AI values for the three NDSRIs.

4. Discussion

Nitrosamines have generally been considered potentially potent mutagens and carcinogens, warranting special consideration as a Cohort of Concern (ICH M7 (R2) 2023). However, NDSRIs associated with pharmaceutical API are generally not expected to be as potent as LMW nitrosamines such as NDEA or NDMA due to MW, steric hindrance, mitigating structural features, and competing metabolism (Thresher et al., 2020; Dobo et al., 2022; Ponting and Foster, 2023). Thus, AIs for NDSRIs should be assessed on a case-by-case basis. The read across and published AIs for NFLX, NDLX and NATX were based on NNK as the comparator compound which has structural elements in common with the three NDSRIs evaluated. However, additional analyses for read across (presented herein) which included the use of physicochemical properties and/or mechanistic data evaluating bond energy of the reactive intermediate indicate that the NDSRIs will not be as potent as NNK. The lower potency of the estimated AIs for these NDSRIs were corroborated empirically using *in vivo* mutation frequency data from transgenic rats administered maximum tolerated doses of each NDSRI.

Current AI-setting strategies in recent guidance from both EMA and FDA employ read across or structure activity relationships or the CPCA method to assign NDSRIs to classes (FDA, 2023; EMA, 2023). The worst-case class used in the CPCA assumes that a NDSRI is as potent as

Table 5
CPCA AI, published[21] and alternate AI values[32] for comparator nitrosamines and NDSRIs.

Nitrosamine or NDSRI	AI based on CPCA (ng/day)	Published AIs (ng/day)	AI based on Phys Chem read across (ng/day)	AI based on QM modeling (ng/day)	AI based on mutation frequency (ng/day)
NDEA	18/26.5	18/26.5	NA	NA	22–100
NDMA	18/26.5	96	NA	NA	60
NNK	18/26.5	100	NA	NA	ND
NFLX	18/26.5	100	537	1140	>5000
NDLX	18/26.5	100	537	1152	>5000
NATX	18/26.5	100	537	1190	>4400

N/A = not applicable. For NDEA, NDMA and NNK the AI are based on carcinogenicity data and these compounds were the basis for the physicochemical read across approach.

small, low molecular weight nitrosamines, with AI limits of 18 or 26.5 ng per day from the EMA and FDA respectively. While a reasonable starting point in the absence of other information, the use of read across methods based only on 2D structure and local similarity or SAR rules based on steric hindrance and/or mitigating structural features local to the nitrosamine generally results in overly conservative estimates of AI. Read across techniques using the most similar 2D structural analogs have been employed for decades, and there have always been challenges with its application (Patlewicz et al., 2014). While chemical structure is associated with potency, small changes in structure can have a large impact on potency.

Traditionally, read-across has involved four key areas of comparison including 1) 2D structural similarity 2) intrinsic physicochemical properties, 3) mechanistic properties and 4) potential metabolism. If there is additional information other than structure and local SAR, it should be used to inform and bolster a read across analysis.

Read across considering physicochemical properties combined with global structural similarity is more likely to be consistent with empirical data (Lester et al., 2023). Use of intrinsic properties of molecules is considered a key part of read across. Evaluation of predicted physicochemical properties such as LogP and solubility for NFLX, NDLX and NATX show that NNK is not the best comparator. For example, a high LogP indicates a high lipophilicity which, in turn, supports the lower predicted solubility of the NDSRIs. In our dataset, all three NDSRIs have high predicted LogP values, consistent with the APIs but not consistent with NNK (Table 2). Such properties are designed into API at the outset (Meanwell, 2011). Large differences in important physicochemical properties such as the Log P between NNK and the NDSRIs suggest that, if present in drug product, the NDSRIs are less likely to be soluble and therefore less likely to be as bioavailable when compared with NNK. Such intrinsic properties support a lower overall potency of NFLX, NDLX and NATX when compared with NNK.

Given that the adverse outcome pathway (AOP) of nitrosamine activation and reactivity is well understood, it is logical to use mechanistic data to interrogate potency of nitrosamines. Modeling and evaluating quantum mechanical (QM) parameters of the nitrosamine activation pathway provides a useful way to assess mechanism. QM modeling is one area that can provide a deeper mechanistic understanding and even be used to predict nitrosamine reactivity (Wenzel et al., 2022). It can model several steps in nitrosamine activation including interaction with P450 and reactive intermediate formation and reactivity. QM assessments (De et al., 2024) for several classes of nitrosamines have shown that QM modeling both supports the principles of the CPCA framework but also highlights gaps and inconsistencies in that framework. Importantly, QM modeling may provide a way to predict potency where the CPCA cannot differentiate the chemistry. Kostal (Kostal and Voutchkova-Kostal, 2023) has published data showing that QM parameters can allow for a binning approach to nitrosamine potency, aligned with potency levels proposed by Bercu et al. (2023a,b) e.g. unknown nitrosamines can be separated into high (AI 26.5 ng/day), medium (AI 150 ng/day) and low (AI $>$ 1500 ng/day) potency groups based on mechanism. In the work described here, the QM modeling showed that the change in stretching vibration frequency reflects the long-range electronic effect on the reactivity. The relative electronic effect of the oxygen atoms at the beta or gamma position, a strong electron-withdrawing group like CF[3], and aromatic group substitutions on the potency of the compounds are reflected in Table 2. A local model of IR frequency as a surrogate for bond dissociation energy was correlated for nitrosamines similar to NDSRIs under evaluation. This analysis showed a high correlation of these two factors ($r = 0.9$) and allowed for local modeling and prediction of AIs for the NDSRIs. While assuming similar metabolism for several of the metabolic steps for nitrosamine activation, including alpha carbon hydroxylation, this analysis supports that these NDSRIs would have lower potency when compared to NNK.

Traditional assessments of carcinogenic risk have been based on tumor data from lifetime bioassays in rodents. These assessments employed linear (non-threshold) low-dose extrapolation of the tumor bioassay data to derive a TD_{50} which, in turn, was used to estimate a dose associated with a theoretical excess cancer incidence of 10^{-5} (ICH M7 (R2) 2023). This animal- and time-intensive approach is not practical or in keeping with 3Rs principles (Hubrecht and Carter, 2019) given the sheer number of impurities that may require assessment. More streamlined studies, such as studies of *in vivo* mutagenicity (proximal to tumor formation via the pathway of nitrosamine carcinogenicity) or the use of other methodology such as *in vivo* duplex sequencing, can provide a mechanistically sound and more efficient risk assessment of nitrosamine impurities. Bercu, Valentine and others have also shown that duplex sequencing is highly consistent with TGR mutation results, providing a way to assess mutation without the use of transgenic animals (Bercu et al. (2023a,b); Valentine et al., 2020).

There is considerable literature data defining the metabolism of the APIs from which these NDSRIs are derived (Mandrioli et al., 2006; Lantz et al., 2003; Yu et al., 2016). These API molecules generally do not undergo alpha carbon hydroxylation as a major metabolic pathway which is associated with formation of reactive intermediates and more predominant for LMW nitrosamines such as NDEA, NDMA or NNK. The principal metabolic pathway via CYP2D6 for these APIs have been described in the literature. By extension, LMW nitrosamines, which are half the molecular size of the NDSRIs, are more likely to undergo such metabolism than NDSRIs. This, higher molecular weight is one factor supporting the lesser mutagenic potency of the NDSRIs when compared with the LMW nitrosamines.

The science of carcinogenicity risk assessment has evolved to incorporate a better understanding of biologic processes. Carcinogenesis is a multifactorial process, and the adverse outcomes pathway (AOP) is not linear (Kobets and Williams 2019; Cho et al., 2022). Not all mutations result in formation of a tumor due, for example, to DNA repair mechanisms and immune surveillance with consequent killing of DNA-damaged cells which supports a threshold-based approach. Furthermore, the mutation frequency in the current TGR studies show a clear threshold of effect.

Regulatory guidance such as the ICH M7 (R2) (2023) and EMA's Assessment Report (2020) were developed prior to the use of mutation as a bonafide surrogate endpoint for carcinogenicity (e.g., Johnson et al., 2021). A mechanism-based risk assessment paradigm using genotoxicity AOPs is a scientifically justified and warranted alternative to the linear, low-dose extrapolation approach based on rodent carcinogenicity data. For nitrosamines, mutation is the relevant and sensitive endpoint for the assessment of carcinogenic risk. Mutation is acknowledged as the key precursor event to nitrosamine-induced carcinogenicity for which the mode of action is well-established; this has been repeatedly demonstrated in numerous scientific studies (e.g., Li and Hecht 2022a,b). The transgenic rodent model is a robust, well-validated model to assess mutagenicity *in vivo* (OECD 488 2022) and is informed by scientific study over many years. The OECD 488-compliant TGR model is the accepted standard to assess mutagenicity *in vivo*. Being an vivo study, metabolic aspects are accounted for and mutational events in relevant tissues, e.g., liver for nitrosamines, can be assessed directly.

The AI derived using the NOEL or BMDL from the *in vivo* mutagenicity data (versus a TD_{50} value) is an appropriately conservative estimate of risk because the mutagenicity endpoint, as a required precursor to carcinogenicity for nitrosamines, is more conservative than a tumor endpoint. This was demonstrated for NDMA and NDEA, where the

[2] FDA 2023, EMA 2023, Bercu 2023.

[3] Calculated using the lower of the NOEL or BMDL value from the Big Blue transgenic data in alignment with the ICH M7(R1) addendum approach. The lowest value listed in mg/kg was divided by 50,000 and multiplied by 50 kg to obtain an AI (e.g. for NATX, 4.4 mg/kg/50,000 *50 kg*1000000 ng/mg = 4400 ng per day). These AI calculations are consistent with those described in M7R2. Instead of a TD_{50}, the NOEL or BMDL are employed.

calculated PDE (permitted daily exposure) based on the rodent cancer bioassay is 1–2 orders of magnitude higher that the PDE based on *in vivo* mutagenicity data (Johnson et al., 2021, Table 4). Furthermore, use of a dose causing no effect (NOEL) as the point of departure is more conservative than using a dose eliciting a 50% tumor rate in rodents (e.g., the TD_{50}). In addition, the BMD analysis, also a well-validated approach to data analysis (Hardy et al., 2017; EPA, 2012), employs all available data as opposed to a single derived TD_{50}, and a BMDL (95% lower limit) provides an additional level of conservatism. While the BMDL approach is more analytically robust than the single-point NOEL value, this analysis used the lower of the two values (NOEL or BMDL) to derive the AI as an additional conservative measure.

The NOELs and BMDL values of the NDSRIs relative to the values for NDMA in Table 4 show that there is at least a 10-100x difference in potency present and support an argument for the NDSRIs being both less potent and not in the ICH M7 (R2) Cohort of Concern. A summary of proposed AI values for the NDSRIs is shown in Table 5 and the *in vivo* mutagenicity data suggests that, even using the most conservative (numerically lowest) estimate of AI, levels as high as 4400 ng/day derived as described in ICH M7 (R2) would be appropriately protective based on a threshold argument.

The approach of using the BMDL derived from *in vivo* mutagenicity data has been employed to determine a regulatory exposure limit for ethylmethane sulfonate (Gocke and Müller 2009; Gocke et al., 2009) and the potent alkylating agents N-methyl-N-nitrosourea (MNU) and N-ethyl-N-nitrosourea (ENU) (Johnson et al., 2014). Since that time, the use of BMDL to derive justifiable human exposure limits has been used in case studies and regulatory submissions with other genotoxic compounds such as benzene, mitomycin C, and bis-chloronitrosourea (e.g., Heflich et al., 2020; White et al., 2020; Ponting et al., 2022).

As aforementioned, apart from the clear scientific rationale for mutagenicity-based assessments to support derivation of AI limits, one must consider the practicality (and feasibility) of conducting TGR studies as opposed to rodent carcinogenicity studies for the plethora of NDSRIs. This approach would decrease use of animals and align with principles of the 3Rs. The quantitative approach using *in vivo* genotoxicity data is particularly relevant where carcinogenicity data are unavailable or of poor quality and when *in vivo* mutagenicity dose-response data display a mechanistically understood response threshold (COM, 2018; Ponting et al., 2022). The data presented herein show that the NDSRIs of fluoxetine, duloxetine and atomoxetine are mutagenic *in vitro* and *in vivo*. However, the *in vivo* mutagenicity data demonstrate that all the NDSRI compounds exhibit a threshold response with NOEL at 5 mg/kg. To put this dose in perspective, the NOEL of 5 mg NFLX/kg is more than 3-fold greater than the highest approved maximum dose of the API, fluoxetine (80 mg or 1.6 mg/kg for a 50-kg adult; USPI).

5. Conclusion

The CPCA published by HAs is a good start in the evaluation of unknown NDSRIs and allows for incorporation of additional data to inform a weight-of-evidence risk assessment. The inclusion of physicochemical properties and mechanistic modeling are important for an informed evaluation of risk. In a well-conducted TGR study, a negative result should serve as qualification of a nitrosamine impurity and positive results should be used to assess relative potency to LMW comparators. For TGR-positive mutagenic substances, risk characterization can be evolved further to derive improved estimates of AI limits based on the *in vivo* mutation data.

It should be noted that the current products which can potentially contain NDSRIs have been on the market for decades, and there has been no signal for increased cancer risk (e.g. fluoxetine). Despite limited analytical power, post-marketing pharmacovigilance has not identified any association between these products and a risk for cancer. This would indicate that the level of risk of NDSRIs in these products does not justify the need for the very low AIs currently recommended by health authorities. Given the potentially severe health risks associated with nitrosamines, a cautious and comprehensive approach is necessary to ensure patient safety while maintaining an adequate supply of medicines to treat diseases with significant morbidity.

Disclaimer

Robert A Jolly, Paul D Cornwell, Jessica Noteboom, Fareed B Sayyed, Bishnu Thapa, and Lorrene A Buckley are employees of and may own shares in Eli Lilly and Company, Inc.

Funding

All funding for this work was provided by Eli Lilly and Company, Indianapolis IN, USA.

CRediT authorship contribution statement

Robert A. Jolly: Writing – review & editing, Writing – original draft, Visualization, Supervision, Methodology, Investigation, Formal analysis, Conceptualization. **Paul D. Cornwell:** Writing – review & editing, Supervision, Investigation, Conceptualization. **Jessica Noteboom:** Validation, Project administration, Methodology, Data curation. **Fareed Bhasha Sayyed:** Writing – original draft, Methodology, Investigation, Formal analysis, Data curation. **Bishnu Thapa:** Formal analysis, Data curation. **Lorrene A. Buckley:** Writing – review & editing, Writing – original draft, Project administration.

Declaration of competing interest

The authors declare that they have no known competing financial interests or personal relationships that could have appeared to influence the work reported in this paper.

Data availability

The data that has been used is confidential.

Acknowledgments

The authors thank David Ackley, Douglas Roepke, Ellen Cannady, Sheroy Minocherhomji and Prashant Desai for their reviews of the manuscript and helpful discussions.

Appendix A. Supplementary data

Supplementary data to this article can be found online at https://doi.org/10.1016/j.yrtph.2024.105672.

References

Agilent Technoliges, 2015a. Transpack Packaging Extract For Lambda Transgenic Shuttle Vector Recovery INSTRUCTION MANUAL Catalog #200220 (400 packaging reactions), #200221 (100 packaging reactions), and #200223 (50 packaging reactions) Revision A.0.

Agilent Technologies, 2015b. λ Select-cII Mutation Detection System for Big Blue Rodents INSTRUCTION MANUAL Catalog #720120 Revision B.0.

Aoki, Y., 2017. Evaluation of *in vivo* mutagenesis for assessing the health risk of air pollutants. Gene Environ. 39, 16. https://doi.org/10.1186/s41021-016-0064-6.

Bercu, J.P., Zhang, Shaofei, Sobol, Zhanna, Escobar, Patricia A., Van, Phu, Schuler, Maik, 2023a. Comparison of the transgenic rodent mutation assay, error corrected next generation duplex sequencing, and the alkaline comet assay to detect dose-related mutations following exposure to *N*-nitrosodiethylamine. Mutat. Res. Genet. Toxicol. Environ. Mutagen 891.

Bercu, J.P., Masuda-Herrera, M., Trejo-Martin, A., Sura, P., Jolly, R., Kenyon, M., Thomas, R., Ponting, D.J., Snodin, D., Tuschl, G., et al., 2023b. Acceptable intakes (AIs) for 11 small molecule N-nitrosamines (NAs). Regul. Toxicol. Pharmacol. 142, 105415 https://doi.org/10.1016/j.yrtph.2023.105415.From.NLM.Publisher.

Bringezu, F., Simon, S., 2022. Salmonella typhimurium TA100 and TA1535 and E. coli WP2 uvrA are highly sensitive to detect the mutagenicity of short Alkyl-N-

Nitrosamines in the Bacterial Reverse Mutation Test. Toxicol Rep 9, 250–255. https://doi.org/10.1016/j.toxrep.2022.02.005. From NLM PubMed-not-MEDLINE.
Burns, M.J., Ponting, D.J., Foster, R.S., Thornton, B.P., Romero, N.E., Smith, G.F., Ashworth, I.W., Teasdale, A., Simon, S., Schlingemann, J., 2023. Revisiting the Landscape of potential small and drug substance related nitrosamines in pharmaceuticals. J. Pharmaceut. Sci. 112 (12), 3005–3011. https://doi.org/10.1016/j.xphs.2023.10.001. Epub 2023 Oct 5. PMID: 37805074.
Cho, E., Allemang, A., Audebert, M., et al., 2022. AOP report: development of an adverse outcome pathway for oxidative DNA damage leading to mutations and chromosomal aberrations. Environ. Mol. Mutagen. 63 (3), 118–134. https://doi.org/10.1002/em.22479.
Committee on Mutagenicity of Chemicals in Food, Consumer Products and the Environment, 2018. Statement on quantitative assessment of genotoxicity data. https://www.gov.uk/government/publications/quantitative-approaches-to-the-assessment-of-genotoxicity-data.
Cross, K.P., Ponting, D.J., 2021. Developing structure-activity relationships for N-nitrosamine activity. Comput Toxicol 20, 100186. https://doi.org/10.1016/j.comtox.2021.100186.
De, S., Thapa, B., Sayyed, F.B., Frank, S.A., Cornwell, P.D., Jolly, R.A., 2024. Quantum mechanical assessment of nitrosamine potency. Chem. Res. Toxicol. 37 (6), 1011–1022.
Dobo, K.L., Kenyon, M.O., Dirat, O., et al., 2022. Practical and science-based strategy for establishing acceptable intakes for drug product N-nitrosamine impurities. Chem. Res. Toxicol. 35 (3), 475–489. https://doi.org/10.1021/acs.chemrestox.1c00369.
EMA European Medicines Agency, 2023. EMA/409815/2020 Rev.20 Questions and answers for marketing authorisation holders/applicants on the CHMP Opinion for the Article 5(3) of Regulation (EC) No 726/2004 referral on nitrosamine impurities in human medicinal products.
EPA United States Environmental Protection Agency. Benchmark Dose Technical Guidance. EPA/100/R-12/001 June 2012. Available at: https://www.epa.gov/sites/default/files/2015-01/documents/benchmark_dose_guidance.pdf.
[EMA] European Medicines Agency, 2020. Nitrosamine impurities in human medicinal products. EMA/369136/2020. Available at: https://www.ema.europa.eu/en/documents/referral/nitrosamines-emea-h-a53-1490-assessment-report_en.pdf.
FDA, 2023. Control of Nitrosamine Impurities in Human Drugs. https://www.fda.gov/regulatory-information/search-fda-guidance-documents/controlnitrosamine-impurities-human-drugs. (Accessed 24 March 2023).
FDA, 2022. Strattera USPI 021411s050lbl.
FDA, 2023a. Prozac USPI 018936 S112lbl. pdf.
FDA, 2023b. Cymbalta USPI 021427s055s057lbl.Pdf.
Fine, Jonathan, Allain, Leonardo, Schlingemann, Joerg, Ponting, David J., Thomas, Robert, Johnson, Georg E., 2023. Nitrosamine acceptable intakes should consider variation in molecular weight: the implication of stoichiometric DNA damage. Regul. Toxicol. Pharmacol. 145, 105505. ISSN 0273-2300.
Finkelshtein, E.I., 1999. The correlation of stretch vibrations frequencies with bond dissociation energies. Application to carotenoids. In: Greve, J., Puppels, G.J., Otto, C. (Eds.), Spectroscopy of Biological Molecules: New Directions. Springer, Dordrecht. https://doi.org/10.1007/978-94-011-4479-7_77.
Frisch, M.J., et al., 2016. Gaussian 16, Revision B.0.1. Gaussian, Inc., Wallingford CT.
Gocke, E., Müller, L., 2009. *In vivo* studies in the mouse to define a threshold for the genotoxicity of EMS and ENU. Mutat. Res. 678 (2), 101–107. https://doi.org/10.1016/j.mrgentox.2009.04.005.
Gocke, E., Ballantyne, M., Whitwell, J., Müller, L., 2009. MNT and MutaMouse studies to define the *in vivo* dose response relations of the genotoxicity of EMS and ENU. Toxicol. Lett. 190 (3), 286–297. https://doi.org/10.1016/j.toxlet.2009.03.021.
EFSA Scientific Committee, Hardy, A., Benford, D., Halldorsson, T., et al., 2017. Update: use of the benchmark dose approach in risk assessment. EFSA J. 15 (1), e04658 https://doi.org/10.2903/j.efsa.2017.4658.
Heflich, R.H., Johnson, G.E., Zeller, A., et al., 2020. Mutation as a toxicological endpoint for regulatory decision-making. Environ. Mol. Mutagen. 61 (1), 34–41. https://doi.org/10.1002/em.22338.
Hubrecht, R.C., Carter, E., 2019. The 3Rs and humane experimental technique: implementing change. Animals 9 (10), 754. https://doi.org/10.3390/ani9100754. PMID: 31575048; PMCID: PMC6826930.
ICH M7(R2), 2023. Assessment and Control of DNA Reactive (Mutagenic) Impurities in Pharmaceuticals to Limit Potential Carcinogenic Risk. ICH. https://database.ich.org/sites/default/files/M7_R1_Guideline.pdf.
Jacobson-Kram, D., Sistare, F.D., Jacobs, A.C., 2004. Use of transgenic mice in carcinogenicity hazard assessment. Toxicol. Pathol. 32 (1_Suppl. l), 49–52. https://doi.org/10.1080/01926230490424761.
Johnson, G.E., Soeteman-Hernández, L.G., Gollapudi, B.B., et al., 2014. Derivation of point of departure (PoD) estimates in genetic toxicology studies and their potential applications in risk assessment. Environ. Mol. Mutagen. 55 (8), 609–623. https://doi.org/10.1002/em.21870.
Johnson, G.E., Dobo, K., Gollapudi, B., et al., 2021. Permitted daily exposure limits for noteworthy N-nitrosamines. Environ. Mol. Mutagen. 62 (5), 293–305. https://doi.org/10.1002/em.22446.
Kobets, T., Williams, G.M., 2019. Review of the evidence for thresholds for DNA-Reactive and epigenetic experimental chemical carcinogens. Chem. Biol. Interact. 301, 88–111. https://doi.org/10.1016/j.cbi.2018.11.011.
Kostal, J., Voutchkova-Kostal, A., 2023. Quantum-mechanical approach to predicting the carcinogenic potency of N-nitroso impurities in pharmaceuticals. Chem. Res. Toxicol. 36 (2), 291–304. https://doi.org/10.1021/acs.chemrestox.2c00380.
Kruhlak, N.L., Schmidt, M., Froetschl, R., Graber, S., Haas, B., Horne, I., Horne, S., King, S.T., Koval, I.A., Kumaran, G., Langenkamp, A., McGovern, T.J., Peryea, T., Sanh, A., Ferreira, A.S., Van Aerts, L., Vespa, A., Whomsley, R., 2024. Determining recommended acceptable intake limits for N-nitrosamine impurities in pharmaceuticals: development and application of the carcinogenic potency categorization approach (CPCA). Regulatory toxicology and pharmacology, volume 150, 2024, lester C, byrd E, shobair M, and yan G. Quantifying analogue suitability for SAR-based read-across toxicological assessment. Chem. Res. Toxicol. 36 (2), 230–242.
Lantz, R.J., Gillespie, T.A., Rash, T.J., Kuo, F., Skinner, M., Kuan, H.Y., Knadler, M.P., 2003. Metabolism, excretion, and pharmacokinetics of duloxetine in healthy human subjects. Drug Metab. Dispos. 31 (9), 1142–1150. https://doi.org/10.1124/dmd.31.9.1142. PMID: 12920170.
Lester, C., Byrd, E., Shobair, M., Yan, G., 2023 Feb 20. Quantifying analogue suitability for SAR-based read-across toxicological assessment. Chem. Res. Toxicol. 36 (2), 230–242. https://doi.org/10.1021/acs.chemrestox.2c00311. Epub 2023 Jan 26. PMID: 36701522; PMCID: PMC9945175.
Li, Y., Hecht, S.S., 2022a. Metabolic activation and DNA interactions of carcinogenic N-nitrosamines to which humans are commonly exposed. Int. J. Mol. Sci. 23 (9), 4559. https://doi.org/10.3390/ijms23094559.
Li, Y., Hecht, S.S., 2022b. Metabolism and DNA adduct formation of tobacco-specific NNitrosamines. Int. J. Mol. Sci. 23 (9), 5109. https://doi.org/10.3390/ijms23095109.From.NLM.Medline.
López-López, J.A., Ayala, R., 2016. Assessment of the performance of commonly used DFT functionals vs. MP2 in the study of IL-Water, IL-Ethanol and IL-(H2O)3 clusters. J. Mol. Liq. 220, 970–982.
Lynch, A.M., Howe, J., Hildebrand, D., Harvey, J.S., Burman, M., Harte, D.S.G., Chen, L., Kmett, C., Shi, W., McHugh, C.F., Patel, K.K., Junnotula, V., Kenny, J., Haworth, R., Wills, J.W., 2024. N-Nitrosodimethylamine investigations in Muta™Mouse define point-of-departure values and demonstrate less-than-additive somatic mutant frequency accumulations. Mutagenesis 39 (2), 96–118. https://doi.org/10.1093/mutage/geae001. PMID: 38183622; PMCID: PMC10928842.
Mandrioli, R., Forti, G.C., Raggi, M.A., 2006. Fluoxetine metabolism and pharmacological interactions: the role of cytochrome p450. Curr. Drug Metabol. 7 (2), 127–133.
Mardirossian, N., Head-Gordon, M., 2016. How accurate are the Minnesota density functionals for noncovalent interactions, isomerization energies, thermochemistry, and barrier heights involving molecules composed of main-group elements? J. Chem. Theor. Comput. 12, 4303–4325.
McCann, J., Gold, Lois Swirsky, Horn, Laura, McGill, R., Graedel, T.E., Kaldor, John, 1988. Statistical analysis of Salmonella test data and comparison to results of animal cancer tests. Mutat. Res. Genet. Toxicol. 205 (Issues 1–4), 183–195. ISSN 0165-1218.
Meanwell, N.A., 2011. Improving drug candidates by design: a focus on physicochemical properties as a means of improving compound disposition and safety. Chem. Res. Toxicol. 24 (9), 1420–1456. https://doi.org/10.1021/tx200211v.From.NLM.Medline.
Moser, I.W., Ashworth, Harris, L., Hillier, M.C., Nanda, K.K., Scrivens, G., 2023. N-nitrosamine formation in pharmaceutical solid drug products: experimental observations. J. Pharmaceut. Sci. 112 (5), 1255–1267.
Nudelman, R., Kocks, Grace, Mouton, Bruno, Ponting, David J., Schlingemann, Joerg, Simon, Stephanie, Smith, Graham F., Teasdale, Andrew, Werner, Anne-Laure, 2023. The nitrosamine “saga”: lessons learned from five years of scrutiny. Organic Process Research & Development Article ASAP. https://doi.org/10.1021/acs.oprd.3c00100.
OECD Organisation for Economic Co-operation and Development, 2022. OECD Guideline for the Testing of Chemicals. Test Guideline 488: Transgenic Rodent Somatic and Germ Cell Gene Mutation Assays. OECD, Paris, France. https://doi.org/10.1787/9789264203907-en.
Oliveiria, A.A., Martins-Avila, C., Ponting, D.J., 2023. Collaborative analysis of complex nitrosamines. The Toxicologist, a Supplement to Toxicological Sciences. Abstract #5063.
Park, H.S., Kang, Y.K., 2019. Which DFT levels of theory are appropriate in predicting the prolyl cis–trans isomerization in solution? New J. Chem. 43, 17159–17173.
Patlewicz, G., Ball, N., Becker, R.A., Booth, E.D., Cronin, M.T., Kroese, D., Steup, D., van Ravenzwaay, B., Hartung, T., 2014. Read-across approaches–misconceptions, promises and challenges ahead. ALTEX 31 (4), 387–396. https://doi.org/10.14573/altex.1410071. PMID: 25368965.
Ponting, D.J., Foster, R.S., 2023. Drawing a line: where might the cohort of concern end? Org. Process Res. Dev. 27 (10), 1703–1713. https://doi.org/10.1021/acs.oprd.3c00008.
Ponting, D.J., Dobo, K.L., Kenyon, M.O., Kalgutkar, A.S., 2022. Strategies for assessing acceptable intakes for novel N-nitrosamines derived from active pharmaceutical ingredients. J. Med. Chem. 65 (23), 15584–15607. https://doi.org/10.1021/acs.jmedchem.2c01498.
Purchase, I.F.H., 1985. A comparison of the potency of mutagenic effect of chemicals in short-term tests with their carcinogenic effect in rodent carcinogenicity studies. In: Vouk, Butler (Ed.), Methods for Estimating Risk of Chemical Injury, Hoel and Peakal.
Schlingemann, J., Burns, M.J., Ponting, D.J., Martins Avila, C., Romero, N.E., Jaywant, M.A., Smith, G.F., Ashworth, I.W., Simon, S., Saal, C., et al., 2022. The landscape of PotentiaSmall and drug substance related nitrosamines in pharmaceuticals. J. Pharmaceut. Sci. https://doi.org/10.1016/j.xphs.2022.11.013.From.NLM.Publisher.
Schmezer, P., Eckert, C., Liegibel, U.M., Klein, R.G., Bartsch, H., 1998. Use of transgenic mutational test systems in risk assessment of carcinogens. Arch. Toxicol Suppl. 20, 321–330. https://doi.org/10.1007/978-3-642-46856-8_29. PMID: 9442305.
Thresher, A., Foster, R., Ponting, D.J., Stalford, S.A., Tennant, R.E., Thomas, R., 2020. Are all nitrosamines concerning? A review of mutagenicity and carcinogenicity data. Regul. Toxicol. Pharmacol. 116, 104749 https://doi.org/10.1016/j.yrtph.2020.104749.

Trejo-Martin, A., Bercu, J.P., Thresher, A., Tennant, R.E., Thomas, R.F., Cross, K., Czich, A., Waese, K., Nicolette, J.J., Murray, J., et al., 2022. Use of the bacterial reverse mutation assay to predict carcinogenicity of N-nitrosamines. Regul. Toxicol. Pharmacol. 135, 105247 https://doi.org/10.1016/j.yrtph.2022.105247.From.NLM.Medline.

Valentine, CC 3rd, Young, R.R., Fielden, M.R., Kulkarni, R., Williams, L.N., Li, T., Minocherhomji, S., Salk, J.J., 2020. Direct quantification of *in vivo* mutagenesis and carcinogenesis using duplex sequencing. Proc. Natl. Acad. Sci. U. S. A. 117 (52), 33414–33425. https://doi.org/10.1073/pnas.2013724117. Epub 2020 Dec 14. PMID: 33318186; PMCID: PMC7776782.

Walker, M., Harvey, A.J.A., Sen, A., Dessent, C.E.H., 2013. Performance of M06, M06-2X, and M06-HF density functionals for conformationally flexible anionic clusters: M06 functionals perform better than B3LYP for a model system with dispersion and ionic hydrogen-bonding interactions. J. Phys. Chem. A 117, 12590–12600.

Wenzel, J., Schmidt, F., Blumrich, M., Amberg, A., Czich, A., 2022. Predicting DNA-reactivity of N-nitrosamines: a quantum chemical approach. Chem. Res. Toxicol. 35 (11), 2068–2084. https://doi.org/10.1021/acs.chemrestox.2c00217. Epub 2022 Oct 27. PMID: 36302168.

White, P.A., Long, A.S., Johnson, G.E., 2020. Quantitative interpretation of genetic toxicity dose-response data for risk assessment and regulatory decision-making: current status and emerging priorities. Environ. Mol. Mutagen. 61 (1), 66–83. https://doi.org/10.1002/em.22351.

Yu, G., Li, G.F., Markowitz, J.S., 2016. Atomoxetine: a review of its pharmacokinetics and pharmacogenomics relative to drug disposition. J. Child Adolesc. Psychopharmacol. 26 (4), 314–326. https://doi.org/10.1089/cap.2015.0137. Epub 2016 Feb 9. PMID: 26859445; PMCID: PMC4876529.

Zhao, Y., Truhlar, D.G., 2008. The M06 suite of density functionals for main group thermochemistry, thermochemical kinetics, noncovalent interactions, excited states, and transition elements: two new functionals and systematic testing of four M06-class functionals and 12 other functionals. Theor. Chem. Acc. 120, 215–241.